Front. Mech. Eng. 2025, 20(4): 28
https://doi.org/10.1007/s11465-025-0840-8

REVIEW ARTICLE

Carbon emission in manufacturing processes: modeling and evaluation

Libin WU[a], Yanbin ZHANG (✉)[a], Mengmeng ZHANG[b], Xin CUI[a], Fan ZHANG[c], Peng GONG[a], Mingzheng LIU[a], Min YANG[a], Yusuf Suleiman DAMBATTA[a,d], Changhe LI[a]

[a] Key Laboratory of Industrial Fluid Energy Conservation and Pollution Control (Ministry of Education), Qingdao University of Technology, Qingdao 266520, China
[b] Qingdao HKC Microelectronics Co., Ltd., Qingdao 266288, China
[c] State Key Laboratory of Ultra-precision Machining Technology, Department of Industrial and Systems Engineering, The Hong Kong Polytechnic University, Hong Kong 999077, China
[d] Department of Mechanical Engineering, Ahmadu Bello University, Zaria 810106, Nigeria
✉ Corresponding author. Email: zhangyanbin1_qdlg@163.com (Yanbin ZHANG)

ABSTRACT Sustainable production depends on the optimization of manufacturing processes. The assessment of carbon emissions in manufacturing is crucial for achieving sustainability. However, a comprehensive systematic framework to reflect the carbon emission regularity of manufacturing processes is currently lacking. This study focuses on the modeling and evaluation of carbon emissions by considering machining processes and multiple factors. First, carbon emission models for machining processes, such as turning, milling, and drilling, are systematically summarized by considering power consumption. Second, the influence of system parameters on carbon emissions is analyzed. Results show that cutting depth exerts a substantial effect on carbon emissions, and material removal rate has minimal influence. Last, the emission reduction mechanism and performance of novel sustainable machining processes are examined to contribute to carbon emission reduction. This study helps in systematically understanding carbon emissions in manufacturing processes, providing support for the further development of sustainable manufacturing.

KEYWORDS sustainable production, carbon emission, manufacturing process, power consumption, novel machining processes

1 Introduction

Since the Industrial Revolution, production activities have been causing severe environmental pollution and the greenhouse effect. Sustainable production and carbon-neutral strategies have been proposed to improve the environment [1]. Carbon reduction is one of the key components of sustainable production. Carbon emission reduction can minimize the negative influence on the environment and reduce the rate of global warming, thereby creating a favorable environment for future sustainable production and development. Carbon emission is an umbrella term and synonymous with greenhouse gas emission. Greenhouse gases are constituents in the atmosphere that facilitate the greenhouse effect. As shown in Fig. 1, greenhouse gases primarily include carbon dioxide (CO_2), methane, and nitrous oxide [2]. Among these gases, CO_2 is the most prevalent, so the total amount of carbon emissions can be measured in terms of CO_2 equivalents [3].

The Fifth Assessment Report of the Intergovernmental Panel on Climate Change (IPCC) indicates that the primary cause of global warming is human activity, particularly industry activity [4]. The total global CO_2 emission from industry activities decreased from 10.02 billion tons in 2019 to 9.77 billion tons in 2020; then, it rose to 10.33 billion tons in 2021 and to 10.44 billion tons in 2022 [5]. As shown in Fig. 1, the industrial sector accounts for 17% of global CO_2 emissions and 37% of the total

Received July 27, 2024; accepted October 30, 2024; online August 18, 2025

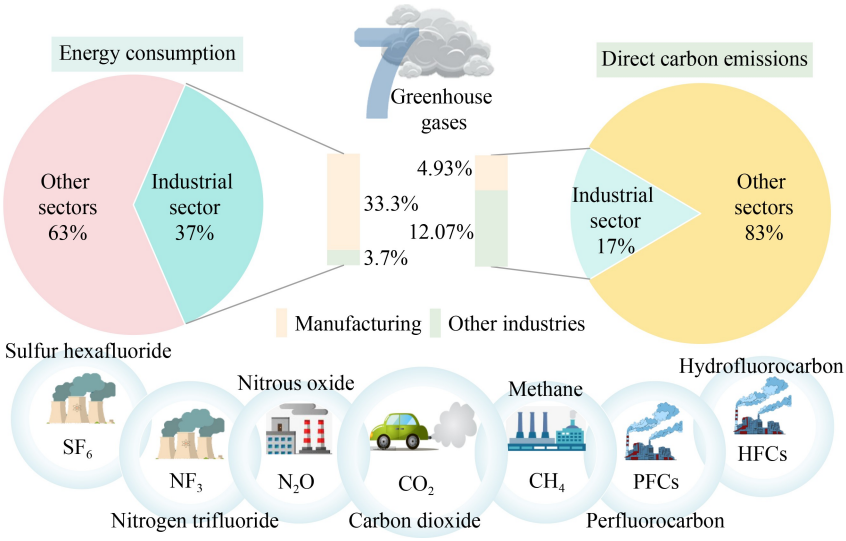

Fig. 1 Seven major greenhouse gases.

energy consumption [6,7]. The manufacturing sector accounts for approximately 29% of the total direct CO_2 emissions from the industrial sector and 90% of the total industrial energy consumption [8,9]. As concerns about climate change intensify, manufacturing, a major part of the industrial sector, is under increasing pressure to reduce its carbon emissions [10]. Against the backdrop of addressing global warming, countries worldwide have reached a consensus regarding carbon emission reduction [11]. Policy interventions, carbon emission trading mechanisms, and carbon taxation mechanisms are the main approaches adopted by countries and regions to achieve emission reduction goals [12].

As shown in Fig. 2, various countries have introduced numerous policies to reduce carbon emissions. For instance, in 1992, nations signed the United Nations Framework Convention on Climate Change to reduce global CO_2 emissions [13]. The Kyoto Protocol, which sets emission reduction targets for parties to the agreement, was signed in Kyoto, Japan, in 1997 [14]. The 2003 UK Energy White Paper titled *Our Energy Future: Creating a Low-Carbon Economy* introduced the concept of a low-carbon economy. In 2004, China approved the Medium and Long-term Special Plan for Energy Conservation, which promotes energy conservation and efficiency across society, thus accelerating the creation of an energy-saving society. The 2009 United Nations Copenhagen Accord imposed considerable pressure on countries to undertake emission reduction obligations, making energy conservation and emission reduction more than just slogans [15]. In the same year, the United States House of Representatives passed the American Clean Energy and Security Act of 2009, which primarily aims to limit carbon emissions. The 2015 United Nations Paris Climate Conference resulted in the Paris Agreement, which seeks to balance climate change mitigation and economic development [16]. In 2020, the European Union implemented the European Climate Law that sets emission reduction targets for 2030. In 2021, China released the Action Plan for Carbon Dioxide Peaking Before 2030, which emphasizes that economic and social development should be based on the efficient use of resources and green, low-carbon development. On May 16, 2023, the European Union officially announced the Regulation Establishing a Carbon Border Adjustment Mechanism (CBAM) and clarified in detail the scope of CBAM, the reporting requirements, and the carbon emission calculations. These policies illustrate the increasing global attention to the issue of carbon emissions [17].

As one of the most important processes in manufacturing, mechanical machining plays a crucial role in emission reduction and energy saving in the manufacturing sector [18,19]. Reducing energy consumption and carbon emissions during the manufacturing process is essential for societal sustainability [20,21]. Carbon emissions from machining include direct carbon emissions, such as fuel combustion and chemical reaction, as well as indirect carbon emissions, such as material consumption, energy consumption, and waste disposal. The proportion of direct carbon emissions is small and can be ignored. Therefore, this study mainly synthesizes the models and mechanisms of indirect carbon emissions.

The first step in reducing carbon emissions in mechanical machining is to analyze the factors influencing carbon emissions during the machining process [22]. The establishment of carbon emission

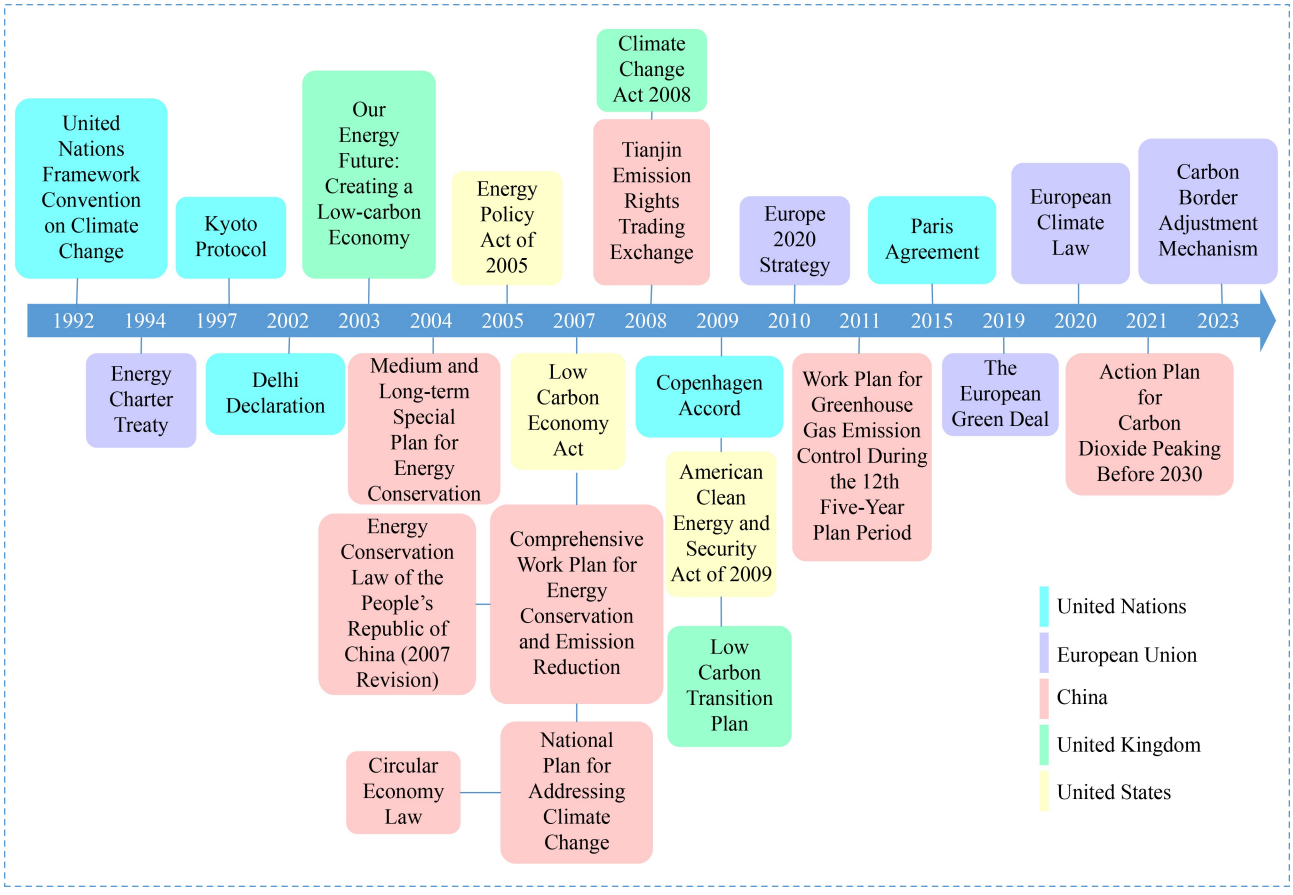

Fig. 2 Policies issued by the United Nations, the European Union, and major countries.

models for mechanical machining can provide a comprehensive understanding of the sources and influencing factors of carbon emissions during the machining process. These models can map the relationship between carbon emissions and factors, such as workpiece material, relevant processes, and cutting parameters, thereby helping implement strategies to reduce carbon emissions during machining. Establishing a low-carbon processing model; simulating and analyzing the dynamic behavior of resources, energy consumption, and environmental emissions in the production process of parts; quantitatively evaluating and identifying high-emission processing units; and performing targeted low-carbon optimization research can help machinery manufacturers improve the utilization rate of energy and materials and reduce CO_2 emissions [23]. However, at present, machining carbon emissions involve complex coupled interactions of multiple variables and parameters, making the mapping between them and related influencing factors challenging.

This study provides a detailed overview of the machining carbon emission model from three aspects: energy consumption, material consumption, and waste disposal. On the basis of the model, the effects of cutting parameters, tool parameters, workpiece parameters, and other factors on carbon emissions are summarized. In addition, in consideration of the shortcomings of traditional machining that uses a large amount of cutting fluid, this study comparatively analyzes the carbon emissions of novel processes, such as dry machining, cryogenic machining, and minimum quantity lubrication (MQL).

2 Carbon emissions in manufacturing

As shown in Fig. 3, the number of publications related to energy and carbon emissions has gradually increased in recent years, particularly after 2013 when a rapid surge in relevant research occurred. Furthermore, carbon emissions from machining processes have garnered considerable attention in developed and developing countries, particularly in China. Manufacturing, as a crucial component of the modern industry, is essential in minimizing resource consumption and carbon emissions during the manufacturing process to alleviate the greenhouse effect. Low-carbon manufacturing has been proposed

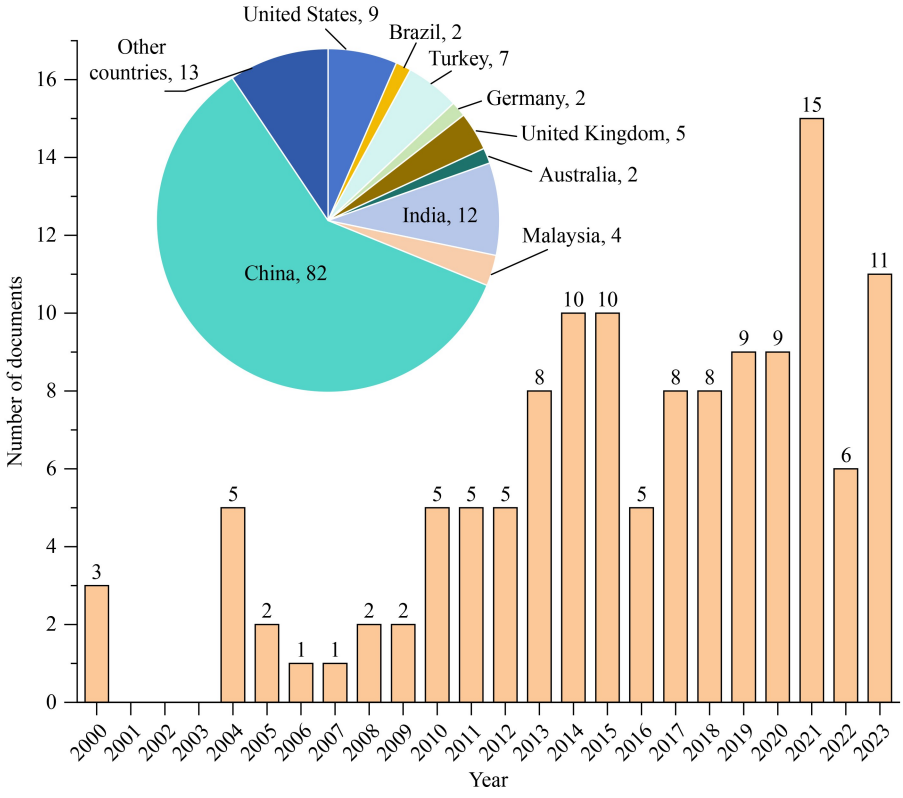

Fig. 3 Literature statistics.

by scholars to reduce carbon emissions from the manufacturing industry.

As shown in Fig. 4(a), Ball et al. [24] introduced the concept of zero-carbon manufacturing. Cao et al. [25] summarized the definition of low-carbon manufacturing as follows: "low-carbon manufacturing is a sustainable manufacturing model that comprehensively considers energy consumption and carbon emissions throughout the entire lifecycle of a product; its goal is to achieve low energy consumption, low emissions, and low pollution during the production, manufacturing, and usage processes of products". Li et al. [26] systematically discussed the connotation of low-carbon manufacturing and the theoretical system of manufacturing and proposed a low-carbon manufacturing technology path based on new-generation information technologies, such as industrial Internet and big data, for China's demand for carbon peaking and carbon neutrality. Low-carbon manufacturing integrates the basic principles of lifecycle analysis and comprehensive consideration of resource and environmental efficiency, and it falls within the realm of green, sustainable manufacturing. The main focus of low-carbon manufacturing is the characteristic of carbon emission reduction. Low-carbon manufacturing can be described as the process of minimizing carbon emissions from the system source and during the manufacturing process [27].

Carbon emission models for machining processes must be established to achieve low-carbon manufacturing. As shown in Fig. 4(b), scholars have developed corresponding carbon emission models for various machining processes. Additionally, energy efficiency, being a crucial aspect of carbon emissions in machining, has been extensively studied by researchers, as indicated in Fig. 4(c). For example, Huang et al. [35] constructed a parametric model that links carbon emissions with laser welding parameters and elucidated the trade-off relationship between carbon emissions and manufacturing value added. Lin et al. [36] proposed a method to quantify carbon emissions throughout the entire turning process in a dry cutting environment and developed a carbon emission model based on the generalized boundary of the machining system. Jiang et al. [37] built a carbon emission model for the laser rapid prototyping manufacturing process. Building on this foundation, they formulated a multi-objective parameter optimization model that targets carbon emissions, powder utilization efficiency, and cladding quality. Zhang et al. [38] studied a carbon footprint optimization control method based on dynamic programming to minimize carbon emissions during the machining process. Meanwhile, Yin et al. [39] introduced a process planning method that integrates economic and environmental factors through a carbon emission function model. This method generates green

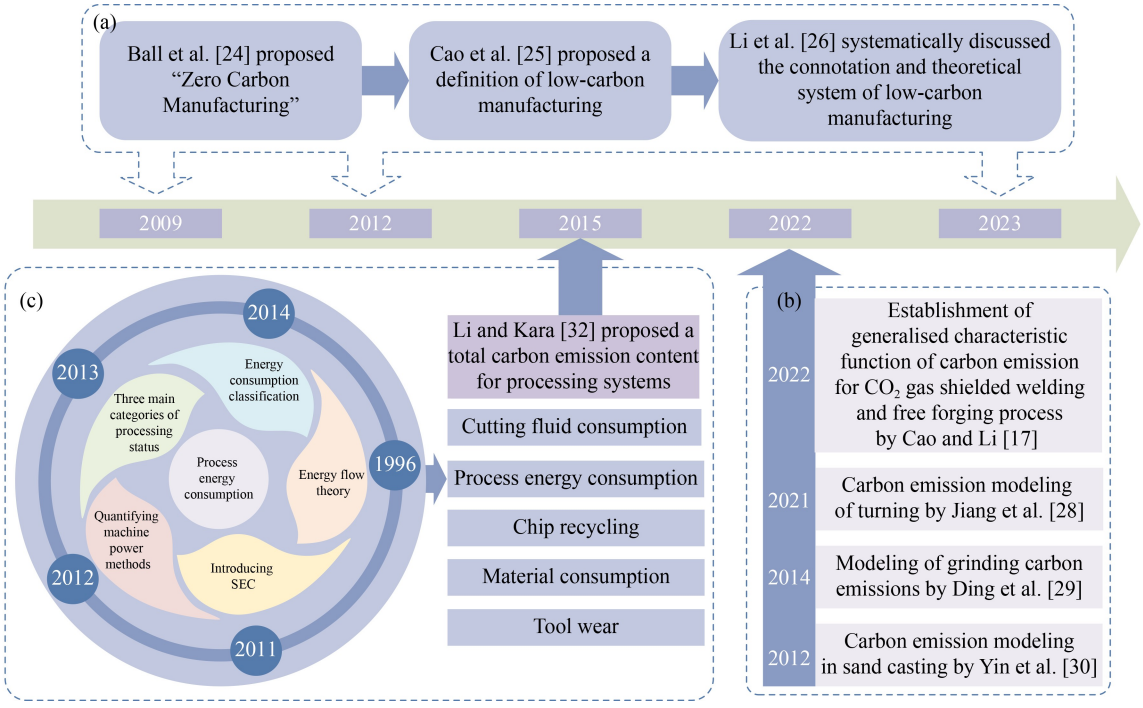

Fig. 4 Development history of carbon emission. (a) Development of definitions [24–26], (b) carbon emission model [17,28–30], and (c) energy consumption [29–34].

and economical process plans, and its feasibility was validated through examples. Cao et al. [40] established a machine tool lifecycle carbon emission model and proposed a quantification method to characterize the carbon emissions of machine tool lifecycles. Sihag and Sangwan [41] proposed an improved micro-level analysis of energy and carbon emissions in value stream mapping for each activity during the machining process. Using milling processes as an example, they demonstrated that the proposed method could optimize the energy efficiency, time efficiency, and carbon emissions of the machining process. In addition, Cao and Li [42] introduced a dynamic simulation method for carbon emissions that considers production disturbances as one of the key factors affecting the carbon emission performance of production systems. Song et al. [43] integrated the principles of life cycle assessment into the carbon emission assessment of machine tool products. They conducted an inventory analysis and calculated carbon emissions during all lifecycle stages, including raw material preparation, product manufacturing, use and maintenance, and transportation.

3 Modeling of carbon emissions in the machining process

3.1 Model frame and content

Mechanical machining is a material removal process during which a large amount of resources is consumed; it generates various waste and emissions that substantially affect the environment [44]. As shown in Fig. 5, the machining boundary employs a blank, machine tool, cutting fluid, and other materials. Electrical energy is inputted into the machine tool, and after the cutting process, chips, waste liquid, waste tools, and other materials are outputted. The cutting process also emits a large amount of heat. On this basis, carbon emissions from machining processes can be grouped into three major categories: carbon emissions from energy consumption, carbon emissions from material consumption, and carbon emissions from waste disposal [45].

The machining carbon emission categories are shown in Fig. 6. Carbon emissions from material consumption include emissions associated with cutting fluid consumption, lubricating oil consumption, tool wear, and fixture wear. Carbon emissions from waste disposal primarily consist of emissions related to the disposal of used tools and cutting fluids, and emissions from chip recycling processes. Carbon emissions from energy consumption encompass dynamic energy usage for cutting, feeding, and other operations, along with the energy consumption inherent in each component of the machine tool. Figure 6 also illustrates that total carbon emissions are influenced by a combination of cutting parameters, tools, lubrication methods, and workpieces. As presented in Fig. 6, carbon emissions

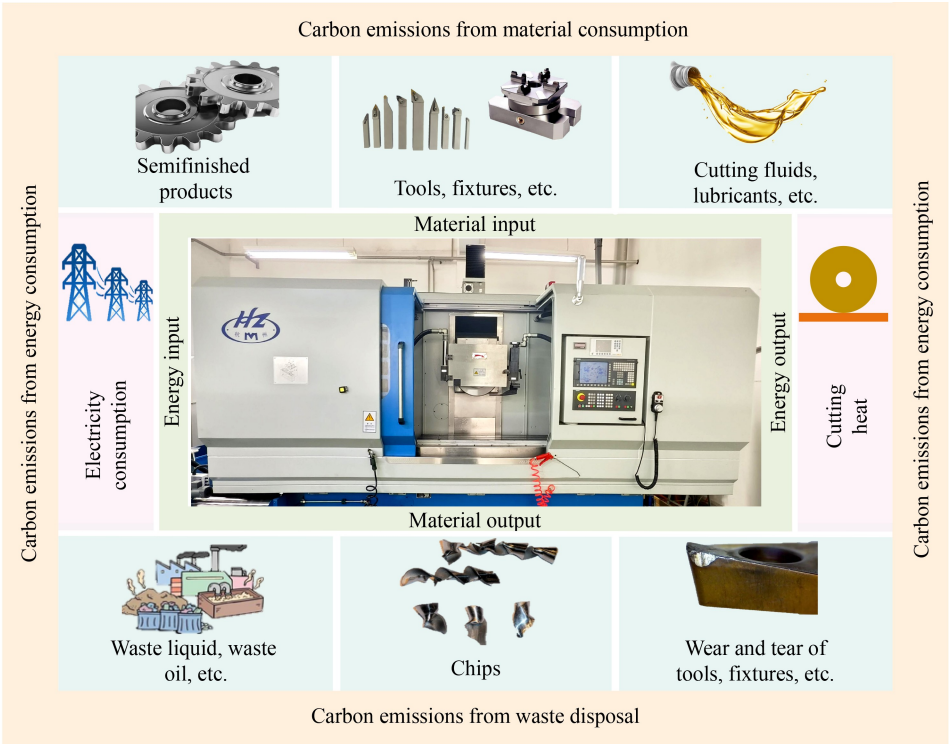

Fig. 5 Machining carbon emission boundary.

from energy consumption are primarily influenced by cutting parameters, such as spindle speed, cutting depth, and feed rate, as well as lubrication methods. Carbon emissions from material consumption are mainly related to workpiece materials, gross size, cutting fluid-related parameters, and lubrication methods. Carbon emissions from waste disposal are primarily associated with the workpiece material and gross size. Notably, lubrication methods can substantially reduce carbon emissions during the machining process by minimizing or eliminating the use of cutting fluids. On this basis, researchers have developed innovative processes, such as cryogenic machining, minimal quantity lubrication, and cryogenic quantity minimal lubrication, which are discussed in Section 5. For ease of calculation, the consumption and recycling processing of tools and cutting fluids are calculated together, and carbon emissions from waste disposal only consider carbon emissions from chip recycling. The total carbon emission model is as follows:

$$\begin{aligned} CE_{\text{total}} &= CE_{\text{elec}} + CE_{\text{material}} + CE_{\text{waste}} \\ &= CE_{\text{elec}} + CE_{\text{c}} + CE_{\text{oil}} + CE_{k} + CE_{j} + CE_{f}. \end{aligned} \tag{1}$$

3.2 Electricity consumption component

The overall energy consumption of computer numerical control (CNC) machine tools is a highly complex system, as depicted in Fig. 7. The total energy consumption of machine tools can be viewed as the sum of the energy consumed by various subsystems [46]. Modern machine tools primarily use electricity as the main power source. The most power-consuming activities of machine tools are spindle rotation and servo-driven axis movements [47], which depend on the cutting load. Other energy requirements come from hydraulic devices, oil pumps, cooling systems, and other auxiliary devices, such as controller units and fans [48]. The multi-source nature of energy consumption and the energy loss characteristics of each device contribute to the complexity of energy consumption in machine tools [33].

The total carbon emissions from electricity consumption are calculated as Eq. (2), where F_{e} represents the carbon emission factor for electricity. Electricity consumption in machine tool machining primarily includes the following components: idle power consumption of the machine tool, cutting power consumption, additional load power consumption, feed power consumption, power consumption of the cooling lubrication system, power consumption of the hydraulic system, and power consumption of other auxiliary systems (e.g., tool change, lighting, display, and chip removal systems). Electricity consumption is determined by the power of the moving parts and the duration of motion [49]. Power

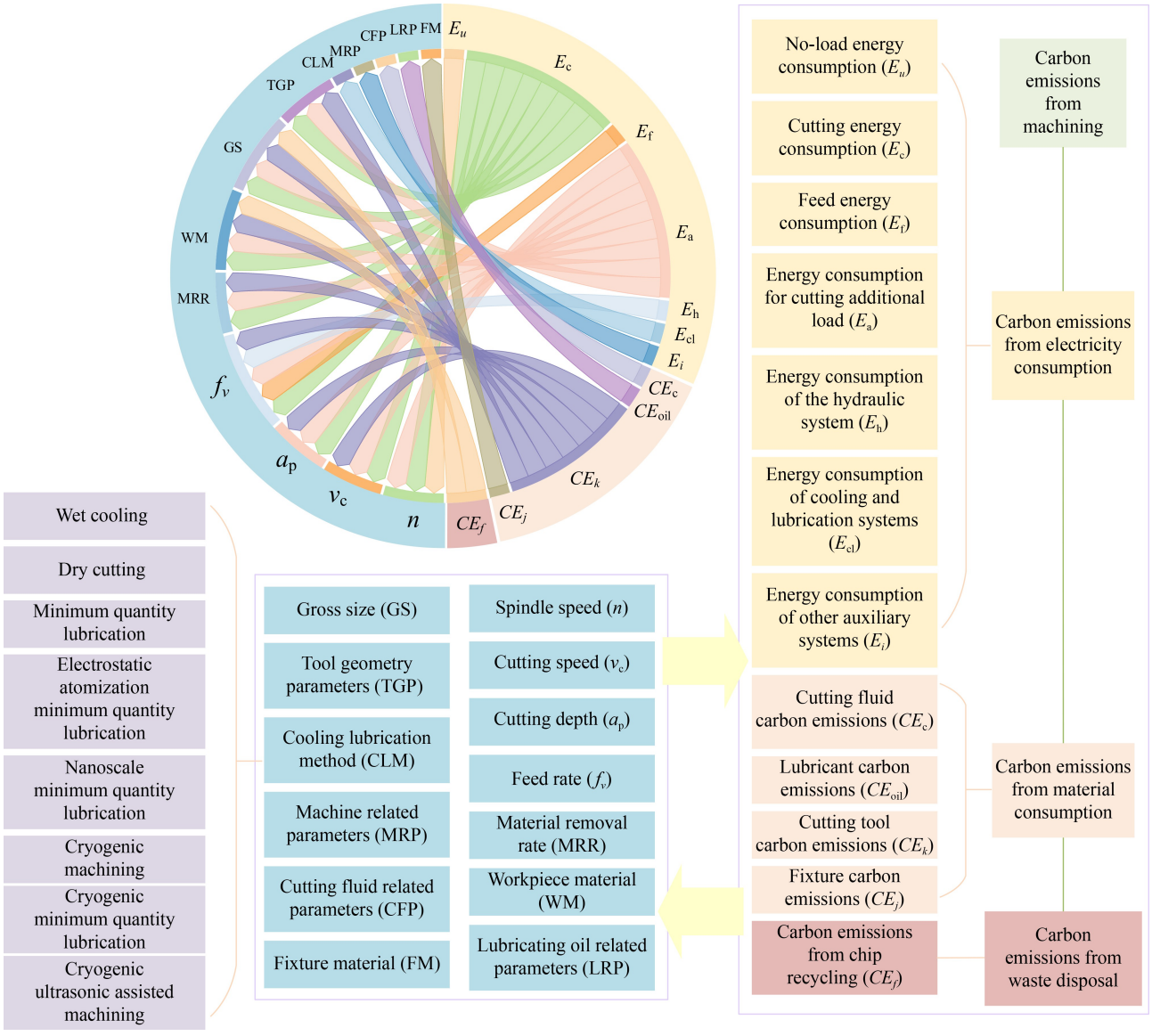

Fig. 6 Carbon emission framework for machining.

is determined by the machining parameters, and understanding the key machining parameters will help improve energy efficiency [50]:

$$CE_{\text{elec}} = (E_u + E_c + E_a + E_f + E_{cl} + E_h + E_i) \cdot F_e. \quad (2)$$

(1) Idle

Idle power consumption of a machine tool, calculated in Eq. (3), refers to the electricity consumed by the motor when it operates without a load; it primarily comprises standby power consumption and air cutting power consumption [51]. It is the energy consumed during machine positioning, tool change, spindle acceleration and deceleration, feed and withdrawal, and other procedures that do not directly relate to workpiece cutting.

$$E_u = P_u \cdot t_u = (P_{u0} + A_1 n + A_2 n^2) \cdot t_u, \quad (3)$$

where P_u (kW) refers to idle power, P_{u0} (kW) is the minimum idle power of the machine tool (standby power), A_1 and A_2 are coefficients related to the spindle speed of the machine tool, t_u is the idle time (min), and n is the spindle speed (r/min).

(2) Cutting

During various machining processes, excess material from the workpiece is removed by the cutting tool, and the electrical energy consumed during this process is the cutting power consumption. As indicated in Eq. (4), the magnitude of cutting energy consumption is related to the machine power during the cutting process and the corresponding cutting time [52].

$$E_c = P_c \cdot t_c = F_c \cdot v_c \cdot t_c, \quad (4)$$

where P_c (kW) is the cutting power, t_c (min) is the

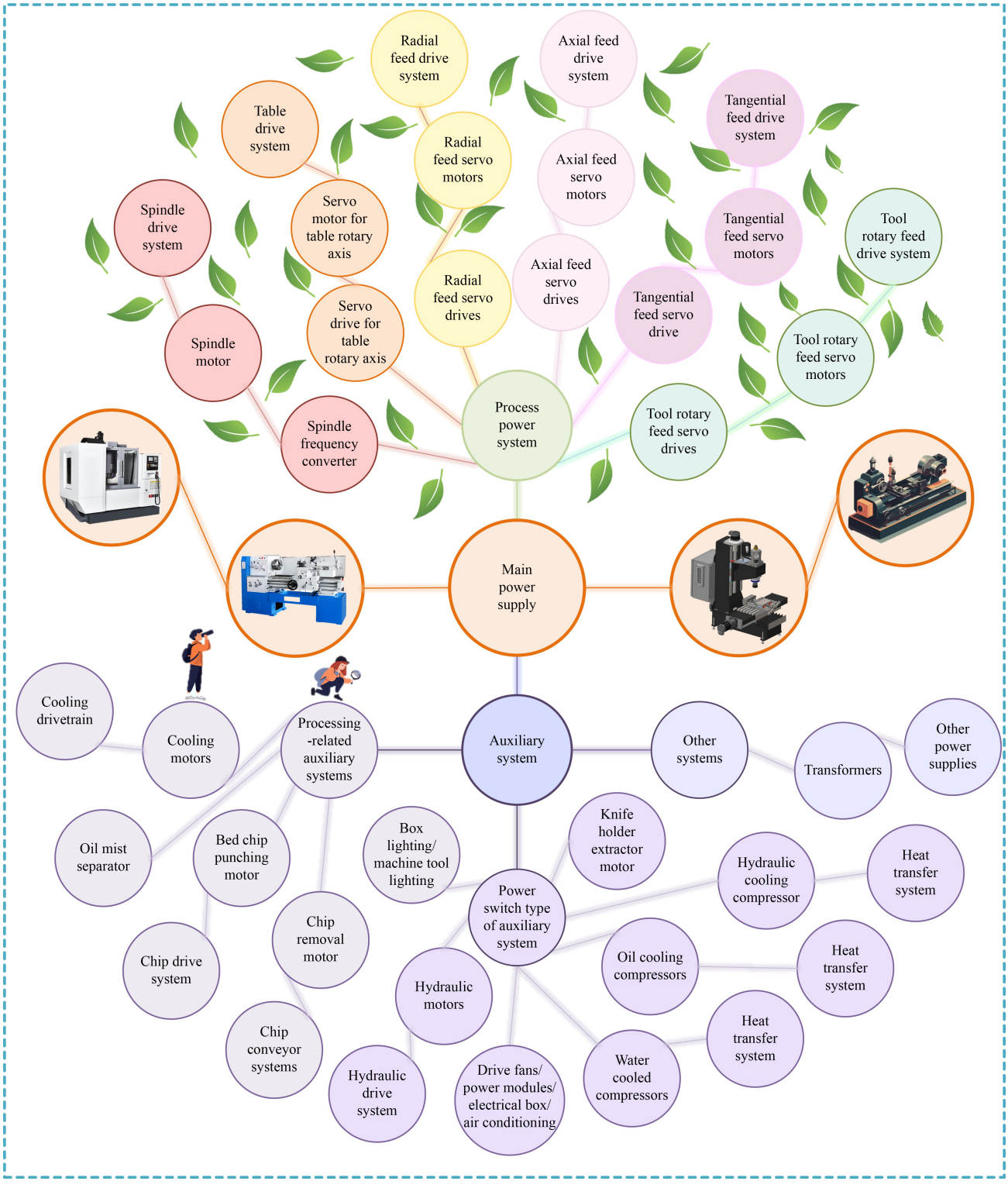

Fig. 7 Energy composition framework for machine tools.

cutting time, F_c (N) is the main cutting force, and v_c (m/min) is the cutting speed.

On the basis of the material removal rate (MRR) cutting power model in Eq. (5), the specific energy consumption (SEC) for machining is defined as the energy consumption required to remove one unit volume of material per unit time (kW/mm^3) [32]. The introduction of SEC simplifies the assessment of energy consumption, and it can be modeled as the inverse function of the MRR, as shown in Eq. (6).

$$P_{\mathrm{c}} = \mathrm{SEC} \cdot \mathrm{MRR} = C_0 + C_1 \cdot \mathrm{MRR} + C_2 \cdot n, \tag{5}$$

$$\mathrm{SEC} = C_0 + \frac{C_1}{\mathrm{MRR}}, \tag{6}$$

where C_0, C_1, and C_2 are inherent coefficients of the machine tool.

The methods for the calculation of cutting time, milling force F_{c1}, and turning force F_{c2} in Eq. (4) are given as Eqs. (7)–(9), respectively [53,54]:

$$t_{\mathrm{c}} = \frac{V}{a_{\mathrm{p}} a_{\mathrm{w}} f_z n z}, \tag{7}$$

$$F_{\mathrm{c1}} = C_{FZ} \cdot a_{\mathrm{p}}^{x_F} \cdot f_z^{y_F} \cdot d_0^{z_F} \cdot Z \cdot a_{\mathrm{w}}^{\alpha_F} \cdot K_F, \tag{8}$$

$$F_{\mathrm{c2}} = C_{FZ} \cdot a_{\mathrm{p}}^{x_F} \cdot f_{\mathrm{c}}^{y_F} \cdot v_{\mathrm{c}}^{n_F} \cdot K_F, \tag{9}$$

where V (mm^3) represents the material removal volume; a_{p} (mm) is the cutting depth; a_{w} (mm) is the cutting width; f_z (mm) is the feed per tooth; z is the number of teeth of the milling cutter; d_0 (mm) is the diameter of the milling cutter; C_{FZ} is the corresponding coefficient; x_F, y_F, z_F, and α_F are constants determined by machining conditions, workpiece material, and tool material; f_{c} is the turning feed rate; and K_F is the correction coefficient.

Grinding power and grinding force (F_{t}) are given by Eqs. (10)–(12) [55]:

$$P_{\mathrm{c}} = F_{\mathrm{t}} v_{\mathrm{s}}, \tag{10}$$

$$F_{\mathrm{t}} = F_{\mathrm{p}} a_{\mathrm{g}}^x f_v^y v_{\mathrm{s}}^z \text{ (surface grinding)}, \tag{11}$$

$$F_{\mathrm{t}} = F_{\mathrm{p}} a_{\mathrm{g}}^x f_{\mathrm{g}}^y f_v^z \text{ (cylindrical grinding)}, \tag{12}$$

where F_{p}, x, y, and z are coefficients and indices related to the grinding process; a_{g} (mm) is the grinding depth; f_v (mm/min) is the feed rate; v_{s} (mm/s) is the grinding speed; and f_{g} (mm) is the grinding feed rate.

The drilling power model is given by Eq. (13) [56]:

$$P_{\mathrm{c}} = f_v \cdot \int \mathrm{d}F_z(z) + \int v(z) \cdot \mathrm{d}F_{\mathrm{t}}(z), \tag{13}$$

where $F_z(z)$ (N) is the cutting force in the Z-axis direction, $F_{\mathrm{t}}(z)$ (N) is the cutting force in the X-axis direction, and $v(z)$ (m/min) is the drilling speed.

(3) Additional load

Additional load power consumption refers to the power of mechanical frictional losses that increase because of the load during cutting operations on the machine tool, as shown in Eq. (14).

$$E_{\mathrm{a}} = P_{\mathrm{a}} t_{\mathrm{c}} = b_{\mathrm{m}} P_{\mathrm{c}} t_{\mathrm{c}}, \tag{14}$$

where P_{a} (kW) is the additional load power and b_{m} is the coefficient of additional load losses.

(4) Feed power

Feed power consumption refers to the total energy consumption of the spindle movement in the X, Y, and Z directions. Feed power is approximately linearly related to the feed rate, as shown in Eq. (16) [57].

$$E_{\mathrm{f}} = \int_{t_{1X}}^{t_{2X}} p_X \mathrm{d}t + \int_{t_{1Y}}^{t_{2Y}} p_Y \mathrm{d}t + \int_{t_{1Z}}^{t_{2Z}} p_Z \mathrm{d}t, \tag{15}$$

$$P_F = C_\varepsilon + K_\varepsilon f_v, \tag{16}$$

where p_X, p_Y, and p_Z (kW) are the feed power in the X, Y, and Z axes, respectively; t_{1X} and t_{2X} are the start and end times of the X-axis feed motion, respectively; t_{1Y} and t_{2Y} are the start and end times of the Y-axis feed motion, respectively; t_{1Z} and t_{2Z} are the start and end times of the Z-axis feed motion, respectively; and K_ε and C_ε are specific coefficients of the motor.

(5) Cooling lubrication

As indicated in Eq. (17), when the machine tool's cooling and lubrication system is in operation, the power consumption of the cooling motor and lubrication pump remains constant. Their electricity consumption depends on the operating time. Here, the switching function $s_i(t)$ is introduced to indicate whether the motor or system is in operation.

$$E_{\mathrm{cl}} = \sum_{i=1}^{n} s_i(t) \cdot p_i \cdot t_i, \tag{17}$$

where n is the number of motors in the cooling and lubrication system, P_i (kW) is the motor output power, and t_i (h) is the motor operating time.

(6) Hydraulic system

The power consumption of the hydraulic system mainly comes from the electrical energy consumed by the movement of tools and worktables, as shown in Eq. (18):

$$E_{\mathrm{h}} = \sum_{q=1}^{m} s_q(t) \cdot p_q \cdot t_q, \tag{18}$$

where m is the number of motion points in the hydraulic system, p_q (kW) is the power consumed at the qth point of the system, and t_q is the working time at the qth point of the system.

(7) Other auxiliary systems

The power consumption of other auxiliary systems mainly includes the energy consumption of lighting, tool changing, control, and other systems. The calculation method is given as Eq. (19).

$$E_i = \sum_{j=1}^{k} s_j(t) \cdot p_j \cdot t_j, \tag{19}$$

where k is the number of energy-consuming subsystems, p_j (kW) is the power of the jth energy-consuming subsystem, and t_j (h) is the operating time

of the jth energy-consuming subsystem.

3.3 Material consumption component

(1) Cutting fluids

In mechanical machining processes, the high temperatures generated in the cutting zone can lead to rapid tool wear, decreased surface integrity, and reduced dimensional accuracy [58]. Therefore, cutting fluids are necessary in most machining processes. Cutting fluids come in various types but are mainly classified into two categories: water soluble (aqueous-based) and non-water soluble (oil-based) [59]. Carbon emissions from cutting fluids mainly include emissions caused by the preparation of pure mineral oil and the disposal of cutting fluid waste [60]. During the cutting process, cutting fluids are typically replaced at fixed intervals [61,62]. Given that the quantity of cutting fluid used cannot be determined, and quantitative analysis cannot be conducted during use, quantitative analysis is performed based on the ratio of usage time to the replacement interval [63]. The calculation method is given as Eq. (20).

$$CE_{\mathrm{c}} = \frac{1}{T_{\mathrm{g}}} \cdot t_{\mathrm{total}} \cdot B_{\mathrm{c}} \cdot (\rho \cdot F_{q1} + F_{q2}), \tag{20}$$

where T_{g} is the replacement interval, B_{c} (L) is the volume of cutting fluid used during the machining process, ρ (kg/cm^3) is the concentration of the cutting fluid, and F_{q1},F_{q2} (kgCO$_2$/L) are the carbon emission factors during the machine tool processing stage and the waste fluid treatment stage, respectively.

Gear hobbing is also important in the mechanical manufacturing industry, and carbon reduction is essential for the sustainable development of gear processing [64]. For the carbon emissions from cutting fluids in gear hobbing, an apportionment calculation method is used; this method distributes the carbon emissions of the cutting fluid evenly to each gear processed. It calculates the carbon emissions of the cutting fluid for machining one gear [65], as shown in Eq. (21).

$$CE_{\mathrm{c}} = \frac{1}{n-x} \sum_{i \in n} \frac{t_i}{T_{\mathrm{c}}} \left(\frac{11}{3} L_{\mathrm{c}} E_{\delta} E_{\gamma} + L_{\mathrm{w}} F_{q2} \right), \tag{21}$$

where T_{c} is the effective recycling period of the coolant in gear hobbing, L_{c} is the amount of coolant recycled in the gear hobbing machine, L_{w} is the volume of cutting fluid wasted during the gear hobbing process, E_{δ} is the energy content of mineral oil, and E_{γ} is the default carbon content of mineral oil.

(2) Lubricant

Many parts of the machine tool require regular maintenance and lubrication with lubricating oil to reduce wear on the machine tool components. The use of lubricating oil also results in carbon emissions. The calculation of carbon emissions from lubricating oil is given as Eq. (22) [29].

$$CE_{\mathrm{oil}} = \frac{T_{\mathrm{s}}}{T_{\mathrm{oil}}} \cdot F_{\mathrm{oil}} \cdot Q_{\mathrm{oil}}, \tag{22}$$

where T_{s} (min) is the spindle rotation time, T_{oil} (min) is the lubricating oil replacement interval, F_{oil} (kgCO$_2$/L) is the carbon emission factor of lubricating oil, and Q_{oil} (L) is the volume of lubricating oil used.

(3) Tools

Tool wear substantially affects a tool's lifespan. It helps estimate the tool's efficiency, total manufacturing costs, and effect on carbon emissions [66]. From an environmental perspective, disposing the worn-out portion of the tool after its service life results in high carbon emissions [67,68]. Tool wear depends on factors such as cutting conditions, workpiece material, and cutting geometry [69,70]. Carbon emissions from tools are calculated using a time-standard allocation method for the machining process over the tools' life cycle. The specific calculation method is given as Eq. (23).

$$CE_k = \frac{t_{\mathrm{c}}}{(N+1)T} F_k m_k, \tag{23}$$

where F_k (kgCO$_2$/kg) is the carbon emission factor of the tool material, m_k (kg) is the mass of the tool, N is the number of times the tool is sharpened, T (min) is the tool life, and t_{c} (min) is the machining time.

For grinding processes, as shown in Eq. (24), the tool is a grinding wheel, and the carbon emissions from the tool are the carbon emissions from grinding wheel wear.

$$CE_k = \frac{V_s}{V_u} m_k \cdot F_k, \tag{24}$$

where V_u is the available volume of the grinding wheel and V_s is the volume of grinding wheel wear.

Tool life calculation is influenced by the tool and workpiece materials as well as the cutting parameters and cutting environment. Tool life calculation for turning tools is given as Eq. (25) [71], and for milling and drilling tools, it is given as Eq. (26) [72].

$$T = \frac{A^{\alpha}}{v_{\mathrm{c}}^{\alpha} f^{\beta} a_{\mathrm{p}}^{\chi}} \cdot p_{\mathrm{c}}, \tag{25}$$

$$T = \frac{C_r}{v_{\mathrm{c}}^{m} f^{n} a_{\mathrm{p}}^{p} a_{\mathrm{w}}^{s}} \cdot p_{\mathrm{c}}, \tag{26}$$

where α, β, and χ are coefficients related to the tool and workpiece materials. A is a coefficient related to cutting conditions. f is the feed per revolution. C_r, m, n, p, and s are coefficients related to tool life and depend on the machining and tool materials.

For gear hobbing, during the mass production of

gears, gear hob cutters wear out continuously during processing. The carbon emissions caused by tool usage during the gear hobbing process are apportioned to each gear. The carbon emissions attributed to the tool during the machining process for the ith gear (i.e., $CE_{i,k}$) are calculated in Eq. (27) [65].

$$CE_{i,k} = \frac{1}{n-x}\sum_{i\in n}\frac{Nt_i}{T_t}F_k m_k, \tag{27}$$

where N is the total number of gear hob cutters, t_i (s) is the time consumed to cut gear i, T_t (min) is the total life of a gear hob cutter, n is the total number of gears machined from the start to the stop of the gear hobbing machine, and x is the number of defective products during the gear hobbing machining.

(4) Fixture

During machining processes on machine tools, fixtures need to be used to secure the workpieces being machined. As shown in Eq. (28), the carbon emissions generated from the use of fixtures during the machining process are mainly due to the wear of the fixtures.

$$CE_j = \frac{t_j}{T_j}(f_j - f_{jc})\cdot G_j, \tag{28}$$

where T_j (h) is the life of the fixture used, f_j (g/kg) refers to the carbon emissions generated from producing the fixture, f_{jc} (g/kg) denotes the carbon emissions from recycling discarded fixtures, and G_j (kg) is the mass of the fixture material.

3.4 Waste disposal component

Carbon emissions from waste disposal mainly come from the cutting recycling process. During actual machining processes, chips can be recycled for secondary use. Their carbon emissions are divided equally between the original system and the recycling system, as shown in Eq. (29). This carbon emission includes carbon emissions from the production of raw materials and the recycling process [73].

$$CE_f = \frac{1}{2}\left[\delta(F^f + F^r)\cdot M_m\right] + (1-\delta)F^f\cdot M_m, \tag{29}$$

where δ is the metal chip recovery rate, F^f ($kgCO_2/kg$) is the carbon emission factor of the raw material for the part, F^r ($kgCO_2/kg$) is the carbon emission factor of the chip recycling process, and M_m (kg) is the mass of chips generated in the process.

For carbon emissions from chips in gear hobbing, the calculation method is similar to that for cutting fluid carbon emissions, where the emissions are apportioned to each gear. The carbon emissions from chip disposal for producing one gear are calculated in Eq. (30):

$$CE_{i,f} = \frac{M_m F^r}{n-x}. \tag{30}$$

This section provides a detailed summary of the carbon emission model for machining processes, which involve turning, milling, drilling, grinding, and gear hobbing. In terms of energy consumption, these processes are roughly the same, with feed energy consumption differing only because of different feed methods. In terms of tooling, cutting fluids, and waste disposal, gear hobbing is modeled using a batch-calculated apportioned modeling approach because gear hobbing is suitable for mass production.

3.5 Carbon emissions from other typical machining processes

(1) Laser welding

Laser welding consists of multiple systems whose carbon emissions have multi-source, multi-stage composite characteristics [74,75]. The sources of carbon emissions from the laser welding process can be traced back to various systems, including the laser generator (CE_{laser}), the chiller (CE_{cool}), the robot (and its control cabinet) (CE_{robot}), the shielding gas (argon) system (CE_{gas}), and auxiliary systems (CE_{aux}) [76,77]. Laser welding's carbon emissions are calculated as Eqs. (31)–(36).

$$CE_{\text{total}} = CE_{\text{laser}} + CE_{\text{cool}} + CE_{\text{robot}} + CE_{\text{gas}} + CE_{\text{aux}}. \tag{31}$$

$$\begin{aligned} CE_{\text{laser}} &= F_{\text{e}}\cdot(E_{\text{ls}} + E_{\text{lst}} + E_{\text{lw}} + E_{\text{lr}}) \\ &= F_{\text{e}}\cdot\Big(\int_0^{t_{\text{ls}}} P_{\text{ls}}(t)\mathrm{d}t + P_{\text{lst}}\cdot t_{\text{lst}} \\ &\quad + \int_0^{t_{\text{lw}}} P_{\text{lw}}(t)\mathrm{d}t + P_{\text{lr}}\cdot t_{\text{total}}\Big). \end{aligned} \tag{32}$$

In Eq. (32), E_{ls}, E_{lst}, E_{lw}, and E_{lr} represent the energy consumption during the laser startup process, standby state, working state, and small peak state, respectively. P_{ls}, P_{lst}, P_{lw}, and P_{lr} correspond to the instantaneous power during the laser startup process, average power in the standby state, instantaneous power during the working state, and average power during the small peak state, respectively. t_{ls}, t_{lst}, t_{lw}, and t_{total} represent the duration of the laser startup process, the standby state time, the welding duration, and the total time of the welding process, respectively.

$$\begin{aligned} CE_{\text{cool}} &= F_{\text{e}}\cdot E_{\text{cool}} = F_{\text{e}}\cdot P_{\text{cool}}\cdot t_{\text{total}} \\ &= F_{\text{e}}\cdot\frac{\int_0^{t_{\text{cl}}} P(t)\mathrm{d}t}{t_{\text{cl}}}t_{\text{total}}. \end{aligned} \tag{33}$$

$$\begin{aligned} CE_{\text{robot}} &= EF_{\text{elec}}(E_{\text{rst}} + E_{\text{rw}}) \\ &= EF_{\text{elec}}\left[P_{\text{rst}}\cdot t_{\text{rst}} + \int_0^{t_{\text{rw}}} P_{\text{rw}}(t)\,\mathrm{d}t\right]. \end{aligned} \tag{34}$$

In Eqs. (33) and (34), P_{cool} represents the average power of the chiller during operation; E_{rst} and E_{rw} denote the energy consumption of the robot in standby and working states, respectively; P_{rst} and P_{rw} correspond to the average power in the standby state and the instantaneous power in the working state, respectively; t_{rst} is the time the robot remains in the standby state; and t_{rw} represents the time during which the robot is in operation.

$$CE_{\text{gas}} = F_{\text{gas}} \cdot q \cdot t_{\text{gas}}. \tag{35}$$

$$CE_{\text{aux}} = F_{\text{e}} \cdot E_i. \tag{36}$$

In Eq. (35), q represents the flow rate of the shielding gas, t_{gas} is the duration for which the shielding gas is activated, and F_{gas} is the carbon emission factor for the material consumption of the shielding gas.

(2) CO_2 shielded welding

CO_2 shielded welding is a gas shielded welding method that uses CO_2 as the shielding gas. During the welding process, CO_2 gas is directly released into the environment, making it a direct source of carbon emissions at the welding site. Additionally, the welding process consumes various materials and electrical energy, indirectly leading to carbon emissions. Therefore, this portion of carbon emissions is considered indirect carbon emissions [78]. The calculation method is shown in Eq. (37).

$$\begin{aligned} CE_{\text{total}} &= CE_{\text{elec}} + CE_{\text{material}} + CE_{\text{p}} \\ &= a_1 \sum_{j=1}^{n} E_{1j} f_j + a_2 \sum_{k=1}^{m} \sum_{j=1}^{n} M_{2k} E_{2j} f_j \\ &\quad + a_3 \sum_{k=1}^{m} \sum_{j=1}^{n} M_{3k} E_{3j} f_j + C_d, \end{aligned} \tag{37}$$

where CE_{p} represents the process carbon emissions; E_{ij} (i = 1,2,3; j = 1,2,…,n) denotes the consumption amount of the jth type of energy considered in the ith category of carbon emissions; f_j is the conversion factor for the jth type of energy, with standard coal used as a unified energy consumption measurement basis; α_1, α_2, and α_3 are the carbon emission factors for energy, material, and process, respectively; M_{2k} and M_{3k} (k = 1,2,…,m) denote the amount of the kth type of material consumed in material and process carbon emissions, respectively; and C_d is the amount of CO_2 gas consumed during the welding process. The direct release of CO_2 gas into the environment is referred to as direct carbon emission.

(3) Sand casting

Sand casting production is a hybrid manufacturing process where carbon emissions can be categorized into five basic types of process-related carbon sources. The five basic sources can be further divided into two major categories: equipment and non-equipment carbon sources. Equipment carbon sources mainly include idle (standby) carbon sources (C_{PC}) and load carbon sources (C_{LC}). Non-equipment carbon sources encompass material consumption carbon sources (C_{MC}), energy consumption carbon sources (C_{EC}), and unintended carbon sources (C_{UC}) [79].

The primary factors influencing carbon emissions from equipment carbon sources include equipment power (idle or load) and time factors. The calculation method is shown in Eqs. (38) and (39).

$$C_{\text{PC}} = P_o t_n F_{\text{e}}. \tag{38}$$

$$C_{\text{LC}} = (P_o + \mu m_e P_w) \cdot t_n \cdot F_{\text{e}}. \tag{39}$$

In Eqs. (38) and (39), P_o represents the equipment's idle or standby power, t_n is the operating time, P_w denotes the additional power per unit weight of the equipment, μ is the power loss coefficient of the equipment, and m_e is the load mass.

The primary factors affecting carbon emissions from non-equipment carbon sources are the carbon emissions from materials, energy, and waste. The basic calculation method is shown in Eqs. (40)–(42).

$$C_{\text{MC}} = \sum_{i=1}^{n} \sum_{k=1}^{l} (E_k^s \cdot U_i) \cdot F_{\text{e}}. \tag{40}$$

$$C_{\text{UC}} = \sum_{i=1}^{n} \sum_{k=1}^{i} (E_k^s \cdot Q_i \cdot \varphi_i) \cdot F_{\text{e}}. \tag{41}$$

$$C_{\text{EC}} = \sum_{i=1}^{n} V_i \cdot F_i. \tag{42}$$

In Eqs. (40)–(42), U_i represents the quantity of the ith type of material consumed, denotes the electricity consumption at the kth processing stage for treating the material or waste, V_i is the quantity of the ith type of energy consumed, F_i represents the carbon emission factor for the ith type of energy, Q_i is the quantity of the ith type of unintended output, and φ_i is the difficulty coefficient for handling the ith type of unintended substance. φ_i can be comprehensively determined based on the waste treatment situation.

(4) Forging

In the forging process, material carbon emissions primarily result from the burn-off of metals, and energy carbon emissions are associated with the electrical energy consumed by equipment during pre-forging treatment, forging, and post-forging heat treatment stages. Given that forging generally does not produce waste, carbon emissions from waste treatment are not calculated in this study [80]. The specific calculation method for forging is given in Eqs. (43)–(45).

$$CE_{\text{material}} = F_{\text{m}} \cdot q_{\text{b}} \cdot m_{\text{f}}. \tag{43}$$

$$CE_{\text{elec}} = F_{\text{e}} \cdot (E_{q1} + E_{q2} + E_q). \tag{44}$$

$$\begin{aligned} E_q &= \int_0^{x_f} F_{\text{forge}}\,\mathrm{d}v \\ &\approx \frac{1}{2}\sum_{i=0}^{N-1} [F_{f0}(x_i + 1) + F_{\text{forge}} x_i] \cdot (x_{i+1} - x_i). \end{aligned} \tag{45}$$

In Eqs. (43)–(45), F_{m} is the carbon emission factor for the forging material, q_{b} represents the burn-off rate of forging, and m_{f} is the mass of forging. E_{q1} and E_{q2} are the electrical energy consumption of the equipment during pre-forging and post-forging heat treatments, and they can be derived from relevant equipment parameters. E_q is the energy consumption during the forging process. F_{forge} represents the forging force, x_f is the total displacement of the hammer head, x_i denotes the displacement during the ith strike, and N is the number of strikes.

3.6 Carbon emission factor

The carbon emission factor refers to the amount of carbon emissions produced per unit of energy during the combustion or use of each type of energy. Carbon emission factors are qualitative parameters because they are related to the production, consumption, handling, or transportation of energy, materials, consumables, or tools. The emission factor method provided in the IPCC guidelines is currently the most widely used greenhouse gas accounting method. It combines information on the extent of human activities, known as activity data (AD), with the emission or removal coefficients that quantify the emissions per unit of activity (emission factor, EF). This relationship can be simply expressed by the formula $E = \text{AD}{\cdot}\text{EF}$.

Carbon emissions from electricity are calculated by multiplying the consumed electricity by the carbon emission factor. This carbon emission factor varies by country or region because it is related to the methods of electricity generation [81]. Peng et al. [82] proposed a method for calculating the comprehensive carbon emission factor for regional power grids in Chinese provinces based on a proportional distribution, and they developed a calculation model for the exchange and consumption of electricity between provinces and regions within provinces. Zhang et al. [83] calculated the full lifecycle carbon emission factor of electricity in China on the basis of ISO 14067 and PAS 2050 standards and recent developments in China's power generation industry, and they made preliminary predictions of the full lifecycle carbon emission factors of electricity in China for 2025 and 2030. Jeswiet and Kara [84] posited that an electrical grid has one or more primary energy sources. The primary energy sources are coal (C), natural gas (NG), petroleum (P), biofuel (B), hydro (H), solar (S), wind (W), geothermal (G), earth (E), wave (Wa), and tidal (T). Each of these can be expressed as a fraction. A grid provides electrical energy and is made up of the sum of fractions of the primary sources multiplied by the conversion efficiency, η, for each energy source. Each electrical power grid has a carbon emission factor, F_{e}. F_{e} can be derived from Eq. (46). The coefficients, namely, 112, 66, and 49, are an unavoidable outcome of combustion and refer to the kilograms of carbon emitted per gigajoule of heat released in each case.

$$F_{\text{e}} = \eta \cdot (112 \cdot x\% \cdot \text{C} + 49 \cdot x\% \cdot \text{N} \cdot \text{G} + 66 \cdot x\% \cdot \text{P}). \tag{46}$$

Many scholars have also conducted research on the calculation of carbon emission factors related to materials. Yu et al. [85] proposed a new method for calculating the carbon emission factor of prefabricated components, which includes analyzing the production process, defining the scope of carbon emissions, identifying carbon emission sources, and establishing a measurement equation for the carbon emissions of prefabricated components. Panagiotopoulou et al. [86] classified carbon emission sources at the process, machine, and system levels and determined the weights of carbon emission factors through sensitivity analysis to identify which carbon emission factor contributes the most to carbon footprint calculation. Hu et al. [87] conducted a systematic literature review to summarize the carbon emission factors associated with railway construction projects. Additionally, some international organizations and regions have already established carbon emission factor databases and are continually improving them. The prevailing carbon emission factors are derived from various sources, including, but not limited to, IPCC, the European Monitoring and Evaluation Programme, the United States Environmental Protection Agency, the Department for Environment, Food and Rural Affairs of United Kingdom, and the Ministry of Ecology and Environment of China [88].

This section provides a detailed summary of carbon emission models for common machining processes, such as turning, milling, drilling, welding, and forging. For machine tool-based processes, such as turning, milling, and grinding, the calculation methods for cutting energy consumption vary depending on the cutting techniques employed, whereas the methods for calculating the inherent energy consumption of machine tools are generally consistent. Regarding the carbon emissions associated with tool wear, various types of tools are utilized in different processes, leading to differences in

calculation methods. In terms of tools, cutting fluids, and waste management, given that gear hobbing is suitable for mass production, a modeling approach that calculates the emissions for the entire production batch and then allocates the results is adopted. Table 1 summarizes the carbon emission calculation formulas for specific aspects of each process. The carbon emissions of welding, casting, and forging processes are calculated separately because of the unique processing methods of these processes.

4 Assessment of the effect of carbon emissions on multiple factors

In machining processes, carbon emissions are influenced by various factors and primarily reflected in cutting parameters, tools, and workpieces. Cutting parameters mainly include MRR, spindle speed, cutting depth, feed rate, and cutting speed [89]. The factors influencing carbon emissions from tools include tool geometry parameters, tool trajectory, and tool material. The factors affecting carbon emissions from workpieces are primarily the workpiece's raw size and material [90].

4.1 Cutting parameters

Jiang et al. [28] found that as spindle speed increases, carbon emissions resulting from energy consumption or cutting fluid usage decrease. However, tool life also decreases as a result, thereby increasing carbon emissions caused by the tool. Therefore, as shown in Fig. 8(c), the overall pattern of carbon emissions follows a quadratic function, exhibiting a minimum value.

The main calculated parameter for cutting speed is spindle speed, and their patterns of change are roughly similar. The effect of cutting speed on carbon emissions and machining time is greater than that of feed rate [53]. Increasing cutting speed to improve machining efficiency does not guarantee low carbon emissions. However, an optimal cutting speed for achieving a balance between machining efficiency and carbon emissions exists [91]. At the same speed, carbon emissions associated with energy consumption from milling are less than those from turning. The main reason is the substantial differences in energy consumption between different machining methods due to variations in cutting forces and tool wear [92].

As shown in Fig. 8(d), the pattern of carbon emissions caused by MRR is similar to that of spindle speed. However, as presented in Eq. (47) [17], the range of MRR variation is limited by small values of feed rate and cutting depth, resulting in a smaller effect on carbon emissions compared with spindle speed.

$$\mathrm{MRR} = f a_{\mathrm{p}} v_{\mathrm{c}}. \tag{47}$$

As shown in Fig. 8(b), with an increase in feed rate, energy consumption carbon emissions and carbon emissions from waste cutting fluid treatment decrease, whereas carbon emissions from tool wear increase. Therefore, a set of cutting parameters corresponding to the minimum carbon emissions for each process stage exists [93].

The influence of cutting depth on carbon emissions during the cutting process is markedly different. Compared with spindle speed and feed rate, cutting depth has the most substantial effect on carbon emissions and machining time [94]. As depicted in

Table 1 Summary of universal and specific formulas

Categorization	Universal formula	Specific formula	
Cutting power consumption	$E_{\mathrm{c}} = P_{\mathrm{c}} \cdot t_{\mathrm{c}} = F_{\mathrm{c}} \cdot v_{\mathrm{c}} \cdot t_{\mathrm{c}}$	Milling	$F_{\mathrm{c1}} = C_{FZ} \cdot a_{\mathrm{p}}^{x_F} \cdot f_z^{y_F} \cdot d_0^{z_F} \cdot z \cdot a_{\mathrm{w}}^{\alpha_F} \cdot K_F$
		Turning	$F_{\mathrm{c2}} = C_{FZ} \cdot a_{\mathrm{p}}^{x_F} \cdot f_{\mathrm{c}}^{y_F} \cdot v_{\mathrm{c}}^{n_F} \cdot K_F$
		Grinding	$P_{\mathrm{c}} = F_{\mathrm{t}} \cdot v_{\mathrm{s}}$
		Surface grinding	$F_{\mathrm{t}} = F_{\mathrm{p}} \cdot a_{\mathrm{g}}^{x} \cdot f_v^{y} \cdot v_{\mathrm{s}}^{z}$
		Cylindrical grinding	$F_{\mathrm{t}} = F_{\mathrm{p}} \cdot a_{\mathrm{g}}^{x} \cdot f_{\mathrm{g}}^{y} \cdot f_v^{z}$
Cutting fluids	$CE_{\mathrm{c}} = \frac{1}{T_{\mathrm{g}}} \cdot t_{\mathrm{total}} \cdot B_{\mathrm{c}} \cdot (\rho \cdot F_{q1} + F_{q2})$	Gear hobbing	$CE_{\mathrm{c}} = \frac{1}{n-x} \sum_{i \in n} \frac{t_i}{T_{\mathrm{c}}} \left(\frac{11}{3} L_{\mathrm{c}} E_{\delta} E_{\gamma} + L_{\mathrm{w}} F_{q2} \right)$
Tools	$CE_k = \frac{t_{\mathrm{c}}}{(N+1)T} F_k m_k$	Turning	$T = \frac{A^{\alpha}}{\nu_{\mathrm{c}}^{\alpha} f^{\beta} a_{\mathrm{p}}^{\chi}} \cdot p_{\mathrm{c}}$
		Milling/drilling	$T = \frac{C_r}{v_{\mathrm{c}}^{m} f^{n} a_{\mathrm{p}}^{p} a_{\mathrm{w}}^{s}} \cdot p_{\mathrm{c}}$
		Grinding	$CE_k = \frac{V_{\mathrm{s}}}{V_u} m_k \cdot F_k$
		Gear hobbing	$CE_{i,k} = \frac{1}{n-x} \sum_{i \in n} \frac{N t_i}{T_t} F_k m_k$
Waste disposal	$CE_f = \frac{1}{2} \left[\delta (F^f + F^r) \cdot M_m \right] + (1-\delta) F^f \cdot M_m$	Gear hobbing	$CE_{i,f} = \frac{M_m F^r}{n-x}$

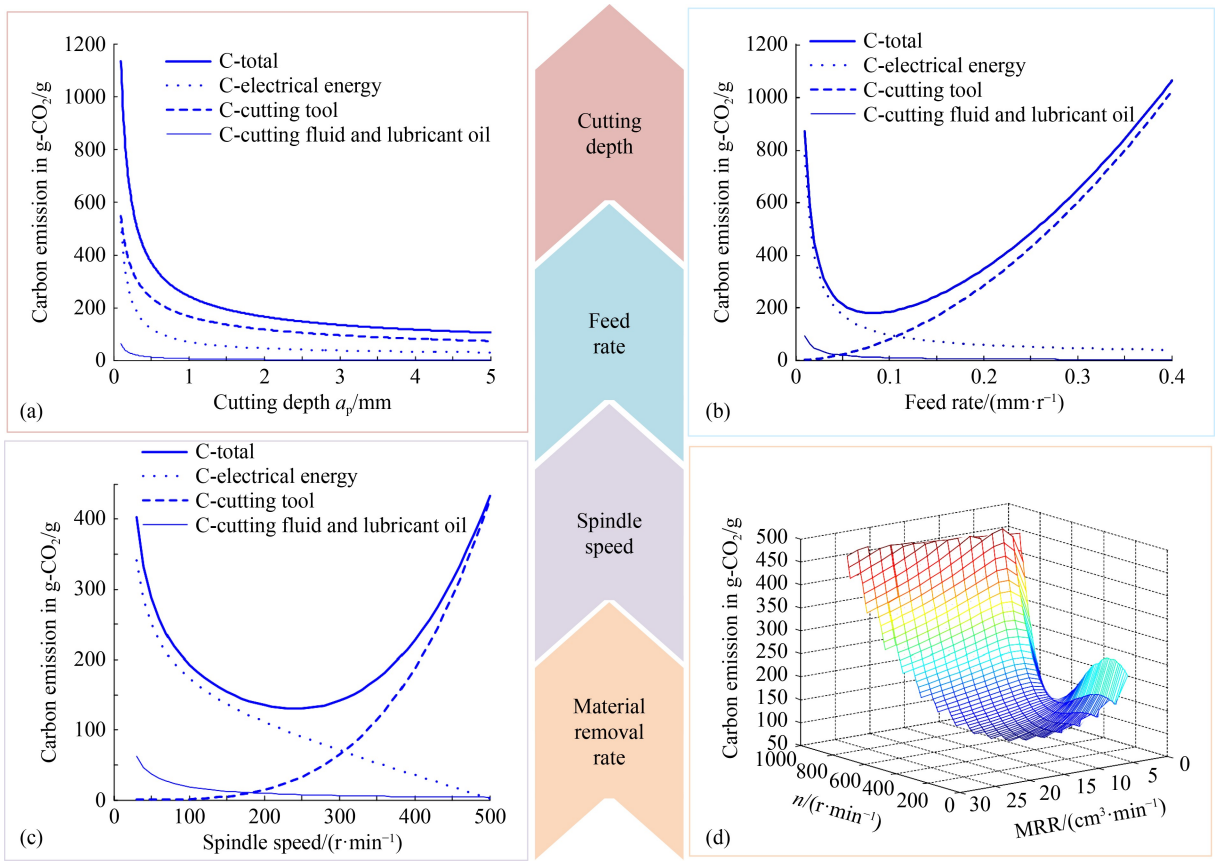

Fig. 8 Effect of cutting parameters on carbon emissions: (a) cutting depth, (b) feed rate, (c) spindle speed, and (d) MRR [28].

Fig. 8(a), the total carbon emissions decrease monotonically with increasing cutting depth. For a given MRR, tool life decreases with increasing cutting depth, leading to increased carbon emissions from tool wear. However, with an increase in cutting depth, machining time decreases, resulting in a reduction in carbon emissions from electrical energy and cutting fluid. Compared with the increase in carbon emissions due to reduced machining time, the increase in carbon emissions from tool wear is minimal. Therefore, at small cutting depths, the total carbon emissions are high, and at large cutting depths, the total carbon emissions are low [95].

4.2 Tool parameters

The factors that affect carbon emissions from tools include tool material, tool geometry angles, diameter, number of teeth, number of sharpening cycles, and quality. Different tool materials exhibit varying cutting energy consumption and tool life under the same operating conditions, leading to different carbon emissions. With regard to tool geometry angles, the rake angle has the greatest effect on cutting forces, with an increase in rake angle resulting in a gradual reduction in cutting forces [96]. Consequently, the electrical energy carbon emissions during cutting also decrease. The selection of different feasible tools can lead to differences in available ranges of cutting parameters, quality, price, precision, and other factors. Each feasible tool has its own unique range of cutting parameters constrained by specific tool and machine specifications.

In terms of tool materials, Tian et al. [97] studied the effect of different tools on carbon emissions and found that when cutting parameters remain constant, machining time does not vary with changes in the tool. However, carbon emissions and costs exhibit substantial variation with different tools. Different tool performance results in different ranges of feasible cutting parameters during the machining process, leading to varying carbon emissions. Selecting appropriate cutting tools during machining processes is advantageous for reducing carbon emissions and machining costs.

4.3 Tool path

The energy consumption of machine tools during operations, such as tool changes and tool path

selection, is influenced by the processing sequence of part features. When the previous feature on the machining sequence differs, changes occur in the tool path and the corresponding tool change plan [98]. This situation results in different values for feed power, feed distance, feed speed, tool change time, and tool change power, leading to variations in total energy consumption during operation [99]. Optimizing tool paths can help reduce energy consumption [100]. Li et al. [101] found that under the same cutting parameter settings, the carbon emissions during conventional parallel milling and streamline milling processes differ. As shown in Fig. 9(a), the energy consumption and carbon emissions during the machining process increase linearly with the increase in tool path. Therefore, selecting appropriate tool paths is crucial for energy conservation and emission reduction efforts.

4.4 Workpiece parameters

The influence of the workpiece on carbon emissions is mainly related to the size of the raw material and the material of the workpiece. Raw material size is one of the parameters used to calculate MRR, and its effect on carbon emissions has been previously discussed. The material of the workpiece affects the electrical energy consumption and tool wear during processing, thereby influencing the carbon emissions generated during the machining process. Generally, compared with cutting ductile materials, cutting brittle materials consumes less electrical energy and results in less tool wear, leading to reduced carbon emissions [90]. In material selection, the following principles can be followed: prioritize the use of renewable materials, choose materials with low energy consumption and pollution, and select materials with good environmental compatibility [102].

With regard to the influence of workpiece material on carbon emissions, Liu et al. [53] investigated the carbon emissions of machining structural steel, gray cast iron, and malleable gray cast iron by using high-speed steel and cemented carbide tools. As depicted in Fig. 9(b), the carbon emissions and machining time of the three materials decrease sequentially, with malleable gray cast iron exhibiting the best machinability. Additionally, the optimal feed rate for high-speed steel tools is higher than that for cemented carbide tools, but the optimal cutting speed is lower. However, compared with high-speed steel tools, cemented carbide tools yield lower carbon emissions and machining time, indicating that cutting speed exerts a more considerable effect on carbon emissions and machining time than feed rate does.

Compared with tools, cutting parameters have a greater influence on carbon emissions during the mechanical machining process. The determination of cutting parameters substantially influences the machining process, and optimizing these parameters is an effective method to improve resource consumption and reduce greenhouse gas emissions in manufacturing [103]. As shown in Fig. 8, among all cutting parameters, cutting depth has the most substantial influence on carbon emissions during the mechanical machining process, and MRR has the least effect. Moreover, the selection of tools, workpiece materials, and machining paths plays a crucial role in carbon emissions during the mechanical machining process. A low carbon footprint should be one of the design constraints when designing products to reduce carbon emissions; this approach is effective for reducing product carbon footprint [104]. During the machining process, the aforementioned factors must be comprehensively considered; appropriate cutting parameters must be set; suitable tools and environmentally friendly materials that are easy to process should be selected; and efficient, low-energy, low-carbon tool paths must be chosen. These measures greatly contribute to reducing carbon emissions during the mechanical machining process.

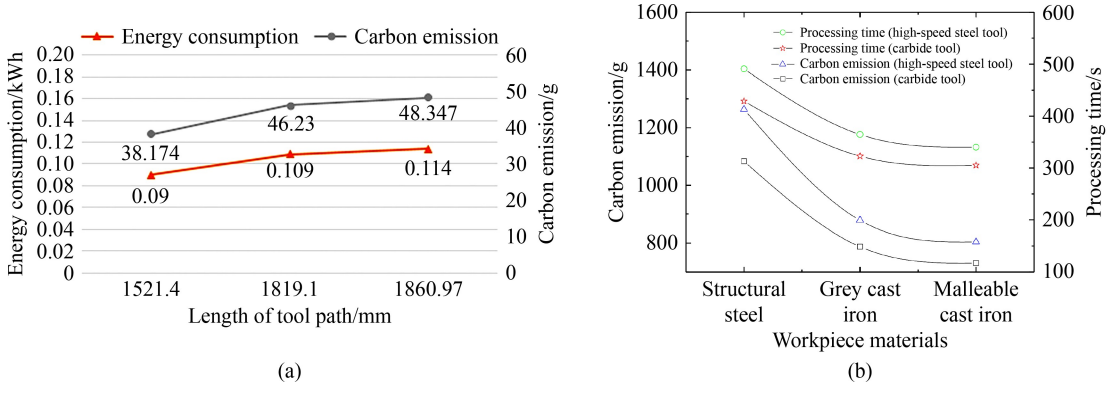

Fig. 9 Carbon emissions from tools and workpieces: (a) effect of toolpath on carbon emissions [101] and (b) effect of workpiece materials on carbon emissions [53].

4.5 Optimization of carbon emissions from machining

Cutting parameters, tools, and workpieces affect machining carbon emissions. As shown in Table 2, to address these factors, scholars have used various methods to optimize carbon emissions during machining. Tian and Yin [105] employed the NSGA-II algorithm to optimize the grinding carbon emission model by optimizing three parameters: grinding wheel linear speed, radial feed rate, and workpiece rotary feed rate. Ic et al. [106] applied the response surface methodology (RSM) to establish a regression model of carbon emission and surface roughness in the turning process and used the expectation function method to obtain the parameter values that minimize surface roughness and carbon emissions. Li and Liu [107] developed a green and efficient milling parameter optimization model to minimize carbon emissions during the milling process. Jiang et al. [108] adopted NSGA-II to solve Pareto boundaries with carbon emission as the optimization objective and used the technique for order preference by similarity to an ideal solution method to rank the Pareto boundaries and determine the optimal combination of cutting parameters. Meanwhile, Yi et al. [63] proposed a carbon emission and machining time turning optimization model on the basis of the proposed system energy boundaries by using the NSGA-II algorithm with cutting speed and feed rate as the limiting conditions. Nguyen et al. [109] used regression analysis to establish a comprehensive model for carbon emissions, specific cutting energy consumption, and surface roughness in turning processes. They optimized the cutting parameters to reduce carbon emissions and energy consumption. The prediction accuracy and optimization performance of these proposed models are shown in Table 3.

However, in machining processes, carbon emissions resulting from energy consumption constitute the majority of the total emissions. Carbon emissions resulting from energy consumption account for approximately 65% of global greenhouse gas emissions [111]. In China, manufacturing energy consumption accounts for about 57% of the total energy consumption, with approximately 16% coming from electricity [112]. Inefficient energy use leads to high carbon emission levels [113]. Machining systems are vast, and machine tools are the most basic energy-consuming equipment in manufacturing. The emissions generated by machine tool electricity cannot be ignored [114]. Many studies have shown that machining system energy efficiency is very low, with only about 30% of energy used for cutting [31]. Gutowski et al. [115] described an example of energy

Table 2 Carbon emission optimization methods

Literature	Process	Optimization parameters	Optimization goals	Methodology
[105]	Grinding	Grinding wheel linear speed, radial feed speed, rotary feed speed of the workpiece	Carbon emission	NSGA-II
[106]	Turning	Cutting depth, cutting speed	Carbon emissions, surface roughness	RSM
[107]	Milling	Spindle speed, axial depth of cut and feed per tooth	Low carbon, profit	Adaptive particle swarm algorithm
[108]	Turning	Cutting depth, feed rate, spindle speed	Carbon emissions, costs	NSGA-II
[63]	Turning	Cutting speed, feed rate	Carbon emissions, processing time	NSGA-II
[36]	Turning	Cutting depth, feed rate, spindle speed	Carbon emissions, processing time, costs	MOTLBO[a)]
[53]	Turning	Cutting depth, feed rate	Carbon emission, working hour	NSGA-II
[54]	Milling	Cutting depth, cutting speed	High efficiency, low energy consumption, low carbon emissions	Weight method

a) MOTLBO: multi-objective teaching–learning-based optimization.

Table 3 Carbon emission model predictions or optimization results in literature

Literature	Process	Experimental method	Carbon emissions (theoretical)/g	Carbon emissions (experimental or optimized)/g	Inaccuracy/ %
[105]	Grinding	Grinding of a certain type of shaft parts with a MORARA MH 3000d CNC grinding machine	23.43	24.41	4.0
[35]	Laser welding	Laser-welded aluminum alloy plate	19.587	20.944	6.4
[55]	Grinding	Grinding 45# steel with the CNC surface grinder MGK7120×6/F	341.29	339.62	0.5
[110]	Milling	SP5040-DK CNC milling machine milling aluminum alloy	0.0313	0.0307	1.9
[78]	CO_2 shielded welding	CO_2 shielded welding using the welding machine model NBC-350TSMI	9.800	9.851	0.5
[37]	Laser additive manufacturing	Cladding 45 steel with LDM4030 powder feeding laser additive equipment	73.5	75.8	3.0

measurement in an automated machining production line and found that only 14.8% of energy is actually used for cutting, with most of the energy being used for the operation of cutting fluid and lubrication systems. Therefore, improving machine tool energy efficiency is crucial in energy conservation and carbon emission reduction.

Many scholars have studied the energy efficiency of machine tool machining processes and employed various approaches to optimize machine tool energy efficiency. Liu et al. [31] proposed an energy flow theory of machining systems and established an energy consumption model for the main drive system of ordinary machine tools. They revealed that the no-load power of the main drive system of machine tools approximates a quadratic function of speed. Jeswiet and Kara [84] introduced the concept of carbon emission signature and established the relationship between carbon emissions and energy consumption. Shi et al. [116] developed an energy flow model for the main drive system of variable-frequency speed-regulated CNC machine tools. They analyzed the power transmission characteristics of the main motor of machine tools and the mechanical transmission system and established dynamic power balance equations for the entire main drive system. Hu et al. [117] built a frequency-based parameter model for the no-load energy of the main drive system of CNC machine tools and analyzed the energy parameter characteristics under no-load operation of machine tools. Balogun and Mativenga [34] categorized machine tool states into three major categories and introduced a ready state between the preparation state and the cutting state. During this stage, abundant energy is required to drive spindle movement to position the tool and workpiece correctly and set the necessary cutting speeds.

5 Carbon emissions from novel processes

Various novel processes have been developed and implemented to mitigate pollution and carbon emissions in the manufacturing industry. Green mechanical processing technology refers to the use of environmentally friendly equipment, processes, and materials to reduce environmental effects while achieving efficient and precise processing during the mechanical processing process. Green processes are based on traditional processes but incorporate advanced technologies to form green processes. Examples include rapid prototyping technology, waste recycling technology, dry machining, and cryogenic machining.

5.1 Dry machining

Compared with dry cutting, traditional wet cutting involves the use of large amounts of cutting fluid, with associated costs comprising approximately 7%–17% of the total manufacturing costs [118]. This situation results in high manufacturing costs, which hinder the sustainable development of related processes [119]. The use of cutting fluids can maximize efficiency, enhance process safety, and improve tool performance and part quality [120]. However, these fluids pose numerous challenges in terms of cost, environmental influence, disposal, and recycling. Examples of these challenges include additional energy, infrastructure, and manufacturing costs; environmental pollution; and threats to workers' health [121].

Innovative technologies have been developed to avoid or minimize the use of cutting fluids, and in some cases, dry machining, that is, machining without the use of cutting fluids, has become feasible [122]. Reducing the use of cutting fluids not only saves costs but also decreases environmental pollution [123]. The environmental performance of dry machining can be broadly reflected in the following aspects: low cost, low resource consumption, low carbon emissions, and absence of toxic substances [124]. However, dry machining still has some drawbacks, such as high cutting temperatures leading to excessive tool wear and short tool life. Additionally, the chips generated during machining cannot be cleared in a timely manner, resulting in surface deterioration [125].

Khanna et al. [66] conducted a comparative analysis of carbon emissions between dry and wet machining processes and found that the total carbon emissions of dry machining are lower than those of wet machining. Wet machining consumes more energy and emits more carbon than dry machining does because of the use of a large amount of cutting fluid, which requires additional power from the motors. Under the same MMR, dry cutting is more energy efficient and environmentally friendly compared with wet cutting [126]. However, dry machining accumulates a large amount of heat in the cutting zone over a certain length of machining, resulting in accelerated tool wear and high carbon emissions from tool wear. Nevertheless, compared with carbon emissions from tool wear in dry machining, the energy consumption carbon emissions caused by the use of cutting fluids in wet machining are higher.

The environmental friendliness of dry machining has been validated in practical applications. Li et al. [127] conducted machining experiments on 192000 automotive transmission gears using a high-speed dry gear hobbing machine and the same batch of gears

using a spray coolant in a traditional gear hobbing machine. They found that high-speed dry gear hobbing consumes 62.5% less electricity and 40% less lubricating oil compared with wet cutting, resulting in 59% less carbon emissions. The carbon emissions from dry gear cutting are much lower than those from traditional wet machining, making the former more environmentally friendly than the latter.

However, Lin et al. [36] found that multi-pass wet machining is more low-carbon than dry machining. Under multi-pass machining conditions, wet cutting allows for high cutting speeds and feed rates, thus reducing the machining time and carbon emissions from tool wear and energy consumption. Despite the carbon emissions generated from the use of cutting fluids, the overall carbon emissions from wet machining are lower than those from dry machining.

5.2 Cryogenic machining

Cryogenic machining involves delivering a low-temperature medium to the cutting zone or within the tool to maintain the cutting area and tool at a low-temperature cooling state for machining [128]. Commonly used cryogenic media include liquid nitrogen (LN_2, −186 °C) and liquid CO_2 (LCO_2, −76 °C) [129]. In comparison with traditional coolant lubrication methods, cryogenic machining does not utilize cutting fluids [130,131]. Nitrogen gas and CO_2 can evaporate into the atmosphere without requiring recovery or treatment, posing no harm to the environment or human health, making cryogenic machining an environmentally friendly machining method [132]. As depicted in Fig. 10(a), during cryogenic machining, LN_2 is sprayed into the cutting area via a nozzle. A calibrated digital K-type thermocouple is installed at the nozzle's tip to monitor the temperature. During the cryogenic machining process, the measured temperature is approximately −175 °C and remains constant throughout the machining operation. An FLIR T640 thermal camera with an accuracy of ±1 °C is utilized to monitor the temperature of the machined surface during actual processing [133]. In machining operations, LN_2 is typically applied to the cutting zone via jetting or immersion to reduce wear, prolong tool life [134], and enhance machining quality with smooth chip evacuation. The cryogenic cooling system of LCO_2 enables accurate and stable flow control, temperature measurement within the pipeline, pressure measurement within the pipeline, and flow rate measurement [135]. LN_2 and LCO_2 exhibit some differences in machining. LN_2's temperature is lower than that of LCO_2, so it enables faster cooling of the tool and workpiece. With regard to the pressure required to maintain a liquid state, LCO_2 requires lower pressure than LN_2 does.

Agrawal et al. [136] conducted turning experiments under conventional wet cooling and N_2 cryogenic cooling conditions and found that deep cold turning at high cutting speeds is a suitable measure to reduce carbon emissions. As shown in Fig. 10(c), compared with wet machining, cryogenic machining exhibits higher material carbon emissions because the coolant (LN_2) used in cryogenic machining evaporates immediately after dissipating heat from the cutting zone and cannot be reused or recycled. Moreover, coolant production generates a large amount of carbon emissions. However, the carbon emissions from chip recovery in cryogenic turning are low, and the energy consumption for waste disposal in cryogenic turning is also low, thereby reducing the overall carbon emissions. Given these factors, cryogenic machining results in lower total carbon emissions compared with wet machining, making it more environmentally friendly.

Khanna et al. [66] conducted a comparative analysis of the carbon emissions of cryogenic and dry machining. As shown in Fig. 10(b), dry cutting generates substantial cutting forces, resulting in high cutting power consumption. In a cryogenic machining environment, energy consumption is considerably reduced, leading to a decrease in carbon emissions. With regard to carbon emissions from tool wear, during cryogenic machining, LCO_2 is sprayed into the cutting zone, remarkably reducing the cutting zone temperature and greatly extending tool life [137]; notably, the carbon emissions generated from tool wear at low temperatures are reduced. Therefore, the total carbon emissions from cryogenic machining are much lower than those from dry machining.

Jamil et al. [138] conducted a comparative study on the sustainability of LN_2 and LCO_2. They found that compared with dry machining, carbon emissions are reduced by approximately 4.58% and 3.57% on average under LCO_2 and LN_2 cooling conditions, respectively. In terms of production energy consumption, LCO_2 requires much less energy compared with LN_2, resulting in lower carbon emissions from LCO_2 processing [139]. Iqbal et al. [140] also demonstrated that the use of a small amount of CO_2 as a coolant during machining does not increase the carbon footprint. Moreover, the preparation of CO_2 as a coolant involves capturing CO_2 from the atmosphere, and during the machining process, CO_2 evaporates back into the atmosphere without increasing the carbon footprint during this process. Therefore, LCO_2 cryogenic machining is sustainable.

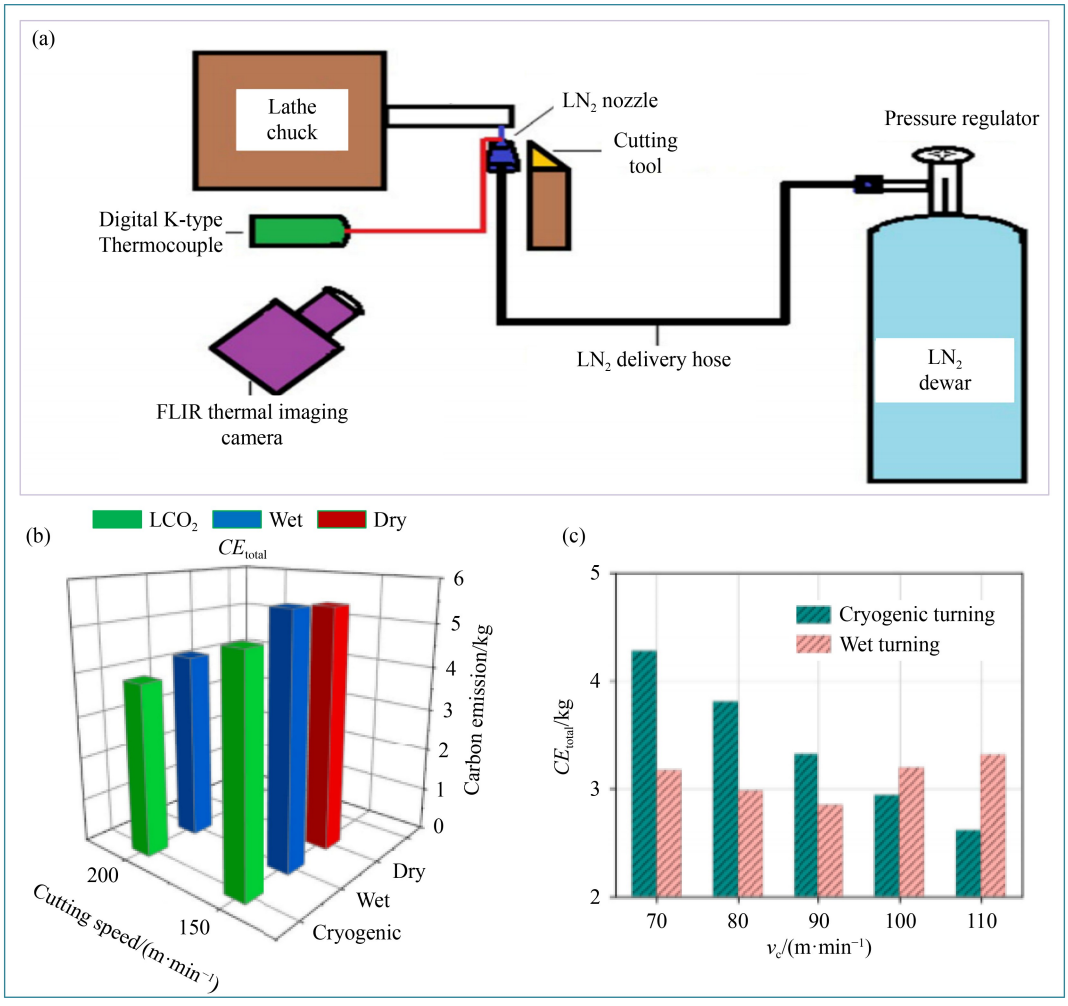

Fig. 10 Cryogenic machining. (a) LN_2 machining equipment [133], (b) machining thin walled α-titanium tubes [66], and (c) cryogenic turning Ti-6AI-4V [136].

5.3 Minimum quantity lubrication

In certain situations where complete removal of the cutting fluid is not feasible because of insufficient air cooling [141], near-dry machining and its enabling technologies, also known as MQL, have been developed. Compared with dry machining, MQL reduces cutting temperatures, tool wear, and surface roughness to a certain extent [142]. MQL mist or aerosol is generated by mixing compressed air with a cutting fluid. A lubricating layer is formed at the tool–workpiece interface, reducing friction and heat generation. This technology involves mixing small amounts of lubricant with high-pressure gas; the lubricant can penetrate the wheel air barrier and reach the grinding zone after mixing and atomization, and the high-pressure gas cools and removes debris [143,144]. MQL utilizes biodegradable plant oils as cutting fluids and thus exerts nearly zero harm to the environment and human health. The consumption of cutting fluid is typically between 10 and 200 mL/h, which is only 1%–10% of that used in traditional flood cooling methods, substantially reducing the usage and disposal costs of cutting fluids.

MQL is more environmentally friendly than dry cutting but slightly less so than cryogenic machining. This conclusion has been validated in the studies conducted by Uysal et al. [145] and Jamil et al. [138]. Under the same cutting conditions, cryogenic and MQL machining experience much lower cutting forces compared with dry machining, with LCO_2 and LN_2 effectively reducing the cutting zone temperature and extending tool life. Consequently, the energy consumption and carbon emissions of cryogenic and MQL machining are lower than those of dry cutting. However, during MQL machining, the power consumption of hydraulic pumps and compressors increases, whereas during cryogenic machining, only the power consumption of compressors is affected. Thus, compared with MQL machining, cryogenic machining produces lower carbon emissions.

The sustainability of MQL has been validated in

practical applications. Zhang et al. [146] developed a micro-droplet MQL device attached to an oil film and conducted data measurements at two user facilities. Under micro-droplet MQL, the oil consumption in the two facilities was reduced by an average of 97.6% relative to the oil consumption under flood cooling, resulting in a yearly CO_2 emission equivalent reduction of 1982 kg. These data indicate that the carbon emissions generated from oil consumption in micro-droplet MQL are much lower than those from traditional flood cooling.

5.4 Electrostatic MQL

MQL's limited penetration and cooling capacity often lead to high heat generation, which accelerates tool wear and compromises the surface integrity of workpieces. As depicted in Figs. 11(a) and 11(b), electrostatic MQL (EMQL) was developed to overcome these limitations. As presented in Fig. 11(c), the cutting fluid is atomized into droplets by high-pressure gas and charged at a copper nozzle. The charged oil droplets are then transported to the cutting zone under the driving force of airflow and electric field [147]. This method combines electrostatic spraying with MQL and uses minimal amounts of lubricating oil (5–20 mL/h), and the charged oil particles enhance the penetration and wetting properties of the cutting zone, thereby improving lubrication performance [148], as shown in Fig. 11(d). Studies have shown that EMQL substantially improves friction and cutting performance; tool life increases by approximately 73% compared with MQL, and lubricant consumption decreases by 67%. Using EMQL can reduce the concentration of floating droplets in the workspace by about 10% compared with MQL, thereby reducing the amount of mist and resulting in minimal harm to human health, reduced environmental damage, and increased environmental friendliness [149,150].

Kashyap et al. [151] analyzed carbon emissions during milling under LCO_2 and EMQL cooling conditions and found that the total carbon emissions from EMQL are 27.69% higher than those from low-temperature LCO_2 machining. The main difference between the two is in carbon emissions from waste disposal, as shown in Fig. 12(c). Similarly, Salvi et al. [152] demonstrated that carbon emissions from waste disposal considerably affect the entire machining process, and dry cutting and LCO_2 cutting environments are more environmentally feasible than EMQL cutting environments. Compared with EMQL machining, low-temperature LCO_2 machining offers longer tool life and lower chip disposal energy

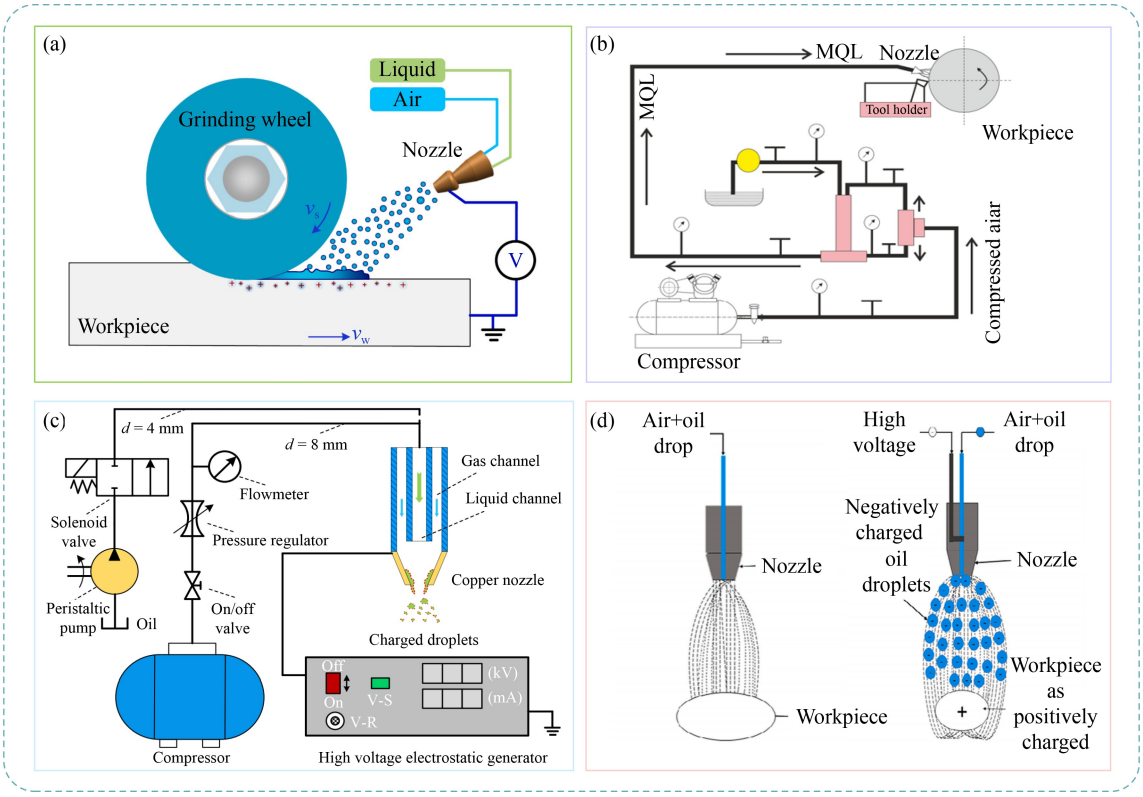

Fig. 11 MQL and EMQL machining principle. (a) MQL principles [147], (b) MQL devices [144], (c) EMQL devices [147], and (d) mechanisms of MQL and EMQL effects [148].

consumption, and the CO_2 gas generated during the machining process can be recovered and reused, resulting in negligible carbon emissions [153].

5.5 Nanofluid MQL

Nanofluid MQL (NMQL), as illustrated in Fig. 12(a), is an innovative lubrication method that combines nano-lubrication with traditional cooling techniques. Its principle involves the addition of a certain proportion of nanoscale lubricants to the coolant, forming a stable and uniform lubricating film. Simultaneously, it effectively reduces the temperature of the coolant, thereby achieving dual effects of lubrication and cooling [154]. NMQL not only inherits the advantages of conventional MQL but also addresses the critical drawback of insufficient heat transfer capability typical of traditional MQL. Furthermore, the excellent tribological properties of nanoparticles enhance the lubrication performance at the wheel/workpiece interface and at the wheel/chip interface, thereby improving the machining accuracy, surface quality, and surface integrity of the workpiece [155]. As depicted in Fig. 12(b), the anti-wear and friction-reducing mechanisms of nanoscale particles at the sliding contact interface can be summarized into four main effects: rolling, film forming, filling and repairing, and polishing. The four effects elucidate the principle of wear reduction by nanoscale particles from different perspectives [156,157].

In the study conducted by Khan et al. [158] that focused on turning Ti-6Al-4V alloy, the carbon emissions during Al-GnP NMQL and low-temperature LN_2 machining processes were investigated. In Fig. 12(d), S_CEe represents the carbon emissions from electrical energy consumption, and S_CEp denotes the total CO_2 emissions per product. The carbon emissions resulting from electrical energy consumption in Al-GnP NMQL are relatively higher than those in LN_2 machining. However, LN_2 production entails high CO_2 emissions, and LN_2 cannot be recycled. For every kilogram of LN_2 synthesized, approximately 0.67 kg of CO_2 is emitted. From the perspective of total carbon emissions, Al-GnP nanofluid-assisted machining yields low carbon emissions.

Ross et al. [139] found that among different methods, dry cutting results in the highest carbon emissions, and NMQL generates the least emissions, as illustrated in Fig. 12(e). The multi-walled carbon nanotubes in NMQL oil reduce friction in the contact area, improve heat dissipation, and thus lower power consumption, and the concentration of nanomaterials substantially reduces the amount of turning associated with machining time. LCO_2 rapidly decreases the heat in the cutting contact area, resulting in short machining time. However, the preparation of LCO_2 entails additional energy consumption and carbon emissions.

By contrast, the findings of Gupta et al. [159], as depicted in Fig. 12(f), indicate that on the average, carbon emissions are reduced by 13.47%, 32.81%, and 49.17% under the cooling and lubrication conditions of MQL, NMQL, and LN_2, respectively, compared with dry turning. The lowest carbon emissions are produced under LN_2 cooling conditions. However, this study did not include the carbon emissions from the preparation process of LN_2.

With regard to the carbon emissions in MQL, EMQL, and NMQL machining processes, with the exception of the calculation methods for carbon emissions from cutting fluid consumption and the electrical energy consumed by the MQL system (E_{MQL}), the other carbon emission calculation methods are similar to those in Section 2. Given that the cutting fluid in MQL, EMQL, and NMQL processes is directly atomized, its recovery does not need to be considered. The carbon emission calculation method is shown in Eqs. (48) and (49).

$$\begin{aligned} CE_{\mathrm{total}} &= CE_{\mathrm{elec}} + CE_{\mathrm{c}} + CE_{\mathrm{oil}} + CE_k + CE_j + CE_f \\ &= (E_u + E_{\mathrm{c}} + E_{\mathrm{a}} + E_{\mathrm{f}} + E_{\mathrm{cl}} + E_{\mathrm{h}} + E_i \\ &\quad + E_{\mathrm{MQL}}) \cdot F_{\mathrm{e}} + CE_{\mathrm{c}} + CE_{\mathrm{oil}} \\ &\quad + CE_k + CE_j + CE_f. \end{aligned} \tag{48}$$

$$CE_{\mathrm{c}} = t_{\mathrm{c}} \cdot Q_{\mathrm{l}} \cdot F_{\mathrm{l}}. \tag{49}$$

In the above equation, Q_{l} represents the flow rate of the cutting fluid, and F_{l} is the carbon emission factor of the cutting fluid.

5.6 Cryogenic MQL

Cryogenic machining inherently limits lubrication characteristics, prompting the development of cryogenic-MQL (CMQL), which combines cryogenic cooling with MQL [160]. When MQL technology is applied in the efficient cutting of difficult-to-machine materials, issues, such as lubrication film rupture and lubrication failure, may occur because of excessively high temperatures in the cutting zone. This problem can be addressed through CMQL, which utilizes the effective cooling of low-temperature cooling media and the anti-friction lubrication properties of lubricating oil. CMQL exhibits excellent lubrication and cooling properties, positively affecting surface integrity and tool life [161]. A recent study indicated that compared with low-temperature cooling alone, the introduction of mixed CMQL reduces surface roughness by 24% and decreases tool wear by 50% [162]. Dry-ice blasting employs compressed air mixed

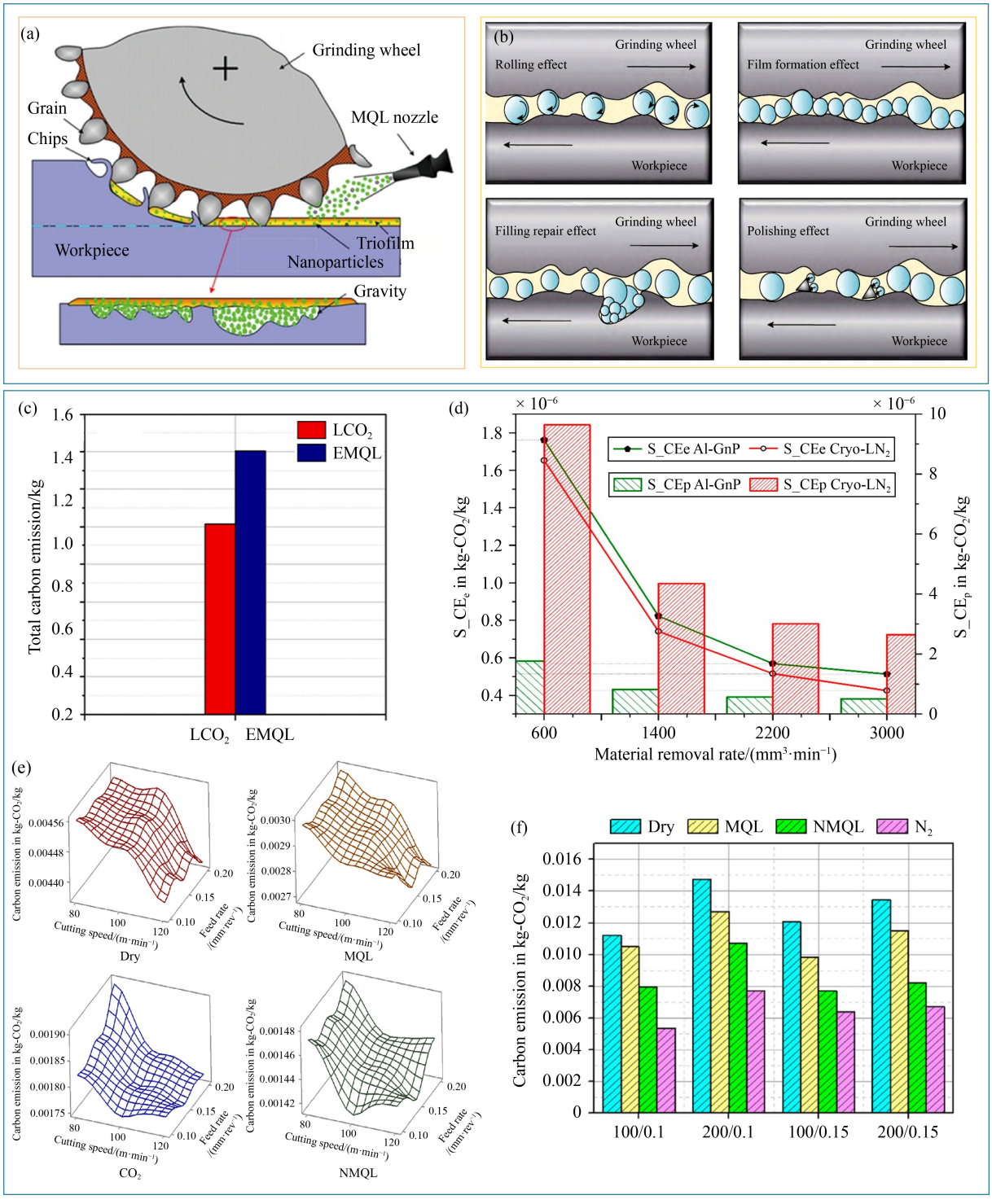

Fig. 12 Comparison of carbon emissions of near-dry machining. (a) NMQL machining principle, (b) lubrication mechanism [156], (c) high-speed drilling [151], (d) turningTi-6Al-4V, (e) turning Monel-400 alloy [139], and (f) turning Inconel-800 alloy [159].

with dry ice to fracture dry ice into small particles, which are then propelled to impact surfaces, serving as a physical means to remove surface contaminants, oils, and dust particles [163]. The lubrication and cooling properties are preserved by combining MQL with dry ice blasting, and timely removal of chips is achieved, thereby enhancing surface quality.

Jamil et al. [164] studied the processability and sustainability of MQL combined with dry-ice blasting. As shown in Fig. 13(a), they found that MQL reduces

energy consumption by 13.3%, and carbon emissions are 54% lower on the average compared with MQL combined with dry-ice blasting, indicating that good processability and sustainability can be achieved with MQL alone. Notably, the manufacturing process of dry ice generates a large amount of energy-related carbon emissions, and the cost of dry ice accounts for nearly 30% of the total machining cost. However, MQL combined with dry-ice blasting reduces surface roughness by 15%, showing high potential for development.

The carbon emission calculation method for the CMQL machining process is shown in Eqs. (50) and (51).

$$\begin{aligned} CE_{\text{total}} &= CE_{\text{elec}} + CE_{\text{c}} + CE_{\text{oil}} + CE_k + CE_j + CE_f \\ &= (E_u + E_{\text{c}} + E_{\text{a}} + E_{\text{f}} + E_{\text{cl}} + E_{\text{h}} + E_i + E_{\text{MQL}} \\ &\quad + E_{\text{ice}}) \cdot F_{\text{e}} + CE_{\text{c}} + CE_{\text{oil}} \\ &\quad + CE_k + CE_j + CE_f. \end{aligned} \tag{50}$$

$$CE_{\text{c}} = F_{\text{l}} \cdot V_{\text{MQL}} + F_{\text{CO}_2} \cdot V_{\text{CO}_2}. \tag{51}$$

In the equations, E_{ice} represents the electrical energy consumed by the cryogenic system during its operation, V_{MQL} denotes the volume of cutting fluid consumed by the MQL system, F_{CO_2} is the carbon emission factor for CO_2, and V_{CO_2} is the volume of CO_2 consumed.

5.7 Cryogenic ultrasonic-assisted machining

The cryogenic ultrasonic-assisted device, as illustrated in Figs. 14(a) and 14(b), introduces ultrasonic vibration to enhance the processability of cryogenic-assisted machining. This intermittent contact between the tool and workpiece induced by ultrasonic vibration positively affects cutting forces [167–169]. Cryogenic ultrasonic vibration assistance retains the benefits of cryogenic assistance while effectively mitigating adverse effects, such as machining hardening [166,170]. This conclusion was validated in the study of Khanna et al. [165]. They analyzed energy consumption and carbon emissions under cryogenic-assisted turning (CAT) and cryogenic ultrasonic-assisted turning (CUAT) conditions, as depicted in Fig. 13(b). They found that compared with CAT, CUAT has lower cutting forces, reduced energy consumption, less tool wear, and lower carbon emissions. This result indicates that introducing ultrasonic assistance into cryogenic turning positively influences cutting processes, making them increasingly environmentally friendly and low carbon.

The carbon reduction potential of processes, including dry machining, cryogenic machining, MQL, NMQL, EMQL, CMQL, and cryogenic ultrasonic-assisted machining is evaluated in this section. These novel processes address the drawbacks of traditional flood cooling methods that utilize large amounts of cutting fluids, substantially reducing carbon emissions associated with the cutting fluid and energy consumption of cooling systems. The primary difference among the carbon emission models of novel and traditional processes lies in the cutting fluids and cooling systems used. A comprehensive literature review was conducted regarding the carbon emissions of these novel processes, and it revealed that scholars mainly performed their calculations on the basis of the general model summarized in Section 3. However, specific carbon emission calculation methods for

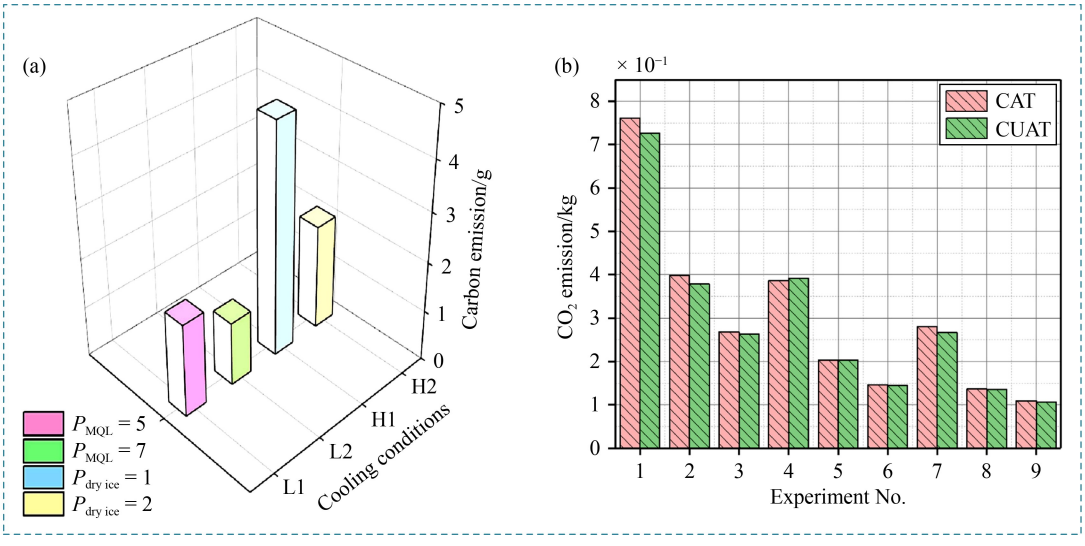

Fig. 13 Mixed processing. (a) MQL–dry ice blasting cooling [164] and (b) cryogenic ultrasonic-assisted processing [165].

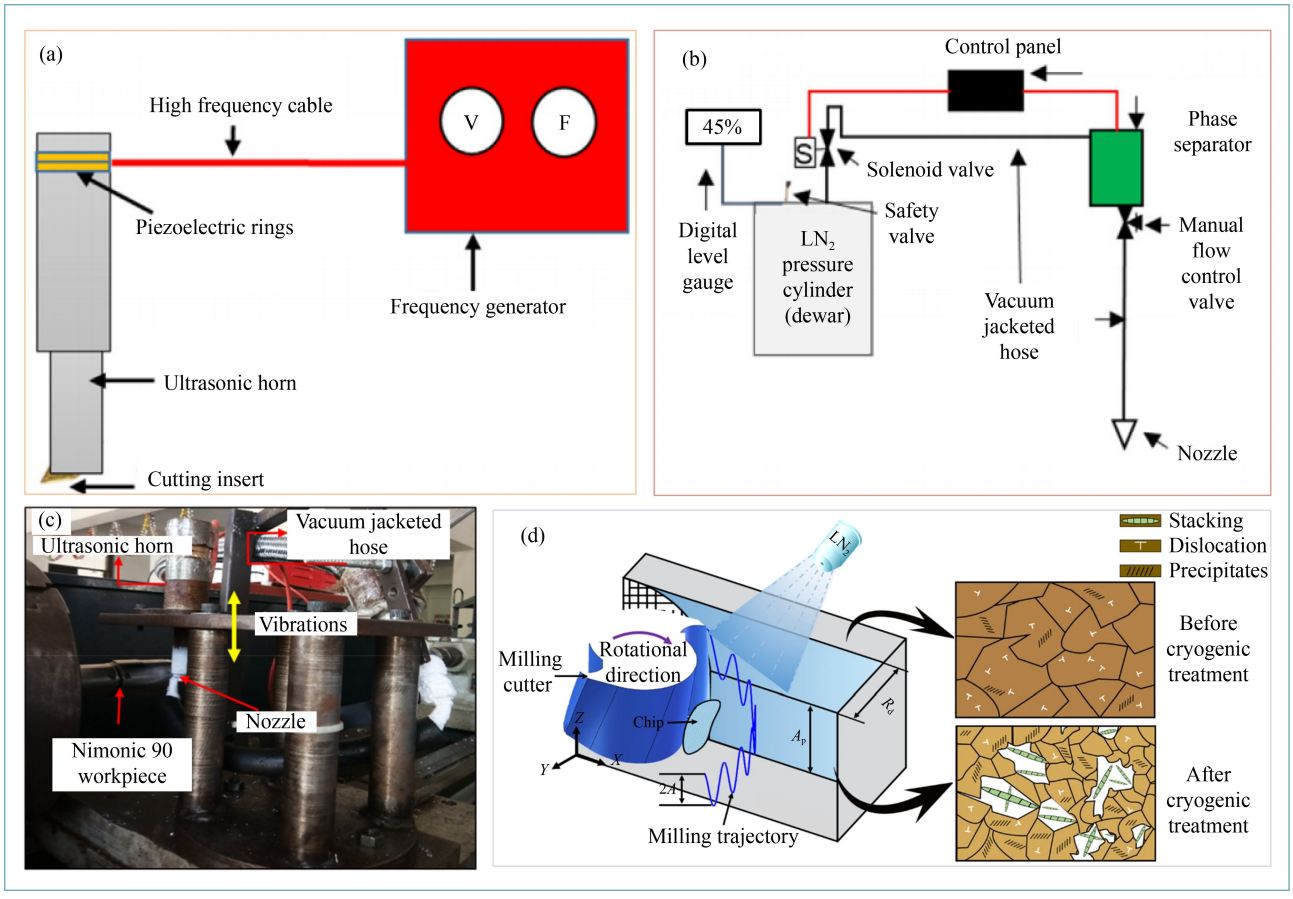

Fig. 14 Principle of cryogenic ultrasonic-assisted machining. (a) Ultrasonic assisted turning process schematic [165,166], (b) CAT process schematic, (c) hybrid turning setup, and (d) cryogenic ultrasonic assisted milling [166].

unique aspects of novel processes, such as MQL equipment and the preparation and release of cryogenic media, have not been established yet. Therefore, this section presents the limited carbon emission models of the novel processes identified in the literature review. Additionally, this section conducts a comparative assessment of the carbon emissions of the novel processes, and the results are presented in Table 4, which shows that the total carbon emissions of most novel processes are higher than those of cryogenic machining. Notably, when the energy consumption associated with the preparation of cryogenic media is excluded, cryogenic machining demonstrates high potential for carbon reduction.

6 Conclusions and prospects

6.1 Conclusions

The following conclusions were obtained after summarizing the carbon emission models in mechanical machining, analyzing the carbon emissions during the machining process, and examining the factors that influence the carbon emissions of machine tool cutting processes.

(1) Carbon emission models for machining processes, such as milling, turning, and grinding, are summarized in this review. Carbon emissions during machining processes comprise three main parts: carbon emissions from electrical energy consumption during cutting, carbon emissions from material consumption, and carbon emissions from waste disposal. Among these, carbon emissions from electrical energy consumption constitute the majority. Furthermore, carbon emissions in machining processes are influenced by various factors, which are categorized into three main groups in this work: cutting, tool, and workpiece parameters. Among them, cutting parameters have the most substantial effect on carbon emissions.

(2) Optimizing cutting parameters is crucial for reducing carbon emissions in machining processes. The effects of five cutting parameters, namely, depth of cut, spindle speed, cutting speed, feed rate, and MRR, on carbon emissions are systematically reviewed in this work, and the optimization methods employed by researchers for these parameters are

Table 4 Comparison of the carbon emissions of novel processes

Reference	Novel process	Major influencing factors	Total carbon emission
[66]	Dry machining[a)]	Tool wear↑	CE_{total}↑
[138]	MQL[a)]	Tool wear↑	CE_{total}↑
		Tool life↓	
[151]	EMQL[a)]	Energy consumption↑	CE_{total}↑
		Cutting fluid consumption↑	
		Recycling of waste tools and cutting fluids↑	
[158]	NMQL[a)]	Energy consumption of N_2 preparation↓	CE_{total}↓
[164]	CMQL[b)]	Energy consumption of dry ice ↑	CE_{total}↑
[165]	CUAT[c)]	Tool wear↓	CE_{total}↓
		Energy consumption↓	

a): Comparison with cryogenic machining. b): Comparison with MQL. c): Comparison with CAT.

summarized. Among these parameters, depth of cut exerts the greatest influence on carbon emissions, followed by feed rate and spindle speed; the least effect is associated with MRR. Furthermore, with the exception of depth of cut, the other parameters have an optimal point where carbon emissions are minimized.

(3) Emerging carbon reduction technologies with remarkable development potential, including dry machining, cryogenic machining, MQL, and several green hybrid processes, are also reviewed. The capabilities of these methods to reduce cutting fluid usage, decrease electrical energy consumption during machining, improve the cutting environment for tools, and extend tool life are highlighted. Reductions in carbon emissions related to cutting fluid consumption, energy usage, and tool wear can be achieved through these technologies. In addition, a comparative assessment of the carbon reduction potential of these novel processes is presented. It reveals that cryogenic machining can reduce carbon emissions by up to 49.17%, and cryogenic machining and its hybrid processes demonstrate substantial carbon reduction potential.

6.2 Prospects

Reducing carbon emissions from the manufacturing industry is essential in mitigating the greenhouse effect and improving the global environment. The development of carbon emission modeling and the improvement and promotion of novel process-related technologies can help reduce carbon emissions from the manufacturing industry. As shown in Fig. 15, to provide direction for scholars to study carbon emission in the manufacturing industry, this study recommends the development of carbon emission modeling, enhancement of carbon emission assessment, promotion of novel processes, and application of carbon emission modeling in four aspects.

(1) Carbon emission models for machining processes involve a multitude of factors and complex influencing mechanisms. Different machining processes are affected by distinct factors and mechanisms, which make the development of accurate carbon emission models challenging. Moreover, current research on carbon emission models concentrates on traditional processes, such as turning, milling, and grinding, and provides little attention to high-pollution, high-energy consumption processes (e.g., electrical discharge machining and laser machining). Therefore, scholars must further investigate the influencing mechanisms of various factors in machining carbon emission models and prioritize the establishment of carbon emission models for special machining processes.

(2) The introduction of carbon tax policies underscores the importance of assessing carbon emissions in machining processes. However, carbon emissions during the cutting operations of machine tools are complex and dynamic. Existing carbon emission models struggle to accurately capture the dynamic nature of carbon emissions that arise from instantaneous changes in cutting power. Furthermore, machining carbon emissions are influenced by various complex factors and mechanisms. As a result of these limitations, current carbon emission models exhibit low assessment accuracy and fail to meet the precision required for contemporary calculations. Therefore, scholars must engage in in-depth research to enhance the accuracy of these models.

(3) Currently, research on the carbon emissions of novel processes is limited and lacks depth. Carbon emission modeling of novel processes is not adequately considered. For example, carbon emissions related to cryogenic media preparation and release and those resulting from the energy consumption of MQL and EMQL equipment also require consideration. Furthermore, the high costs of these novel processes restrict

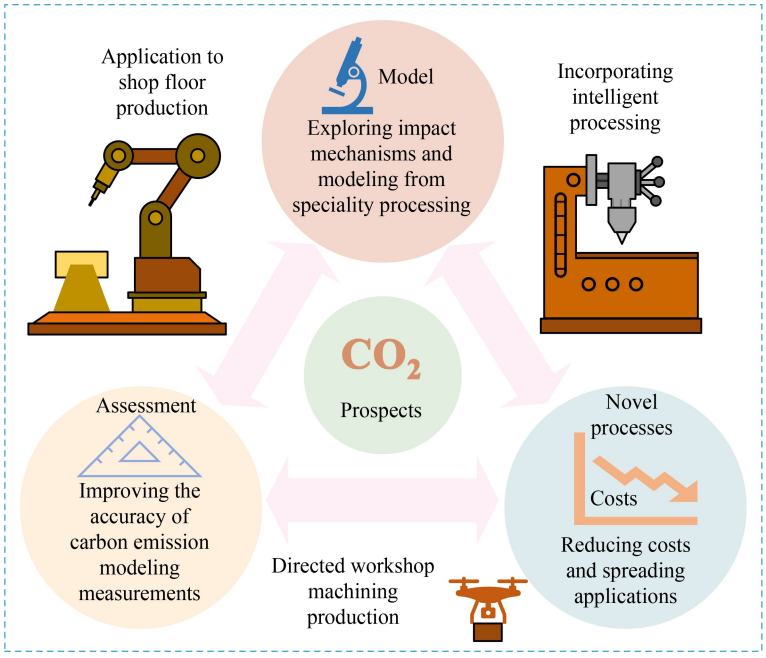

Fig. 15 Prospects for carbon emissions from manufacturing.

their application in production. However, the environmental benefits of novel processes far surpass those of traditional methods. Therefore, future work should focus on continuing in-depth research on modeling the carbon emissions of novel processes, reducing the processing costs of novel processes, promoting the application of green processes in production, and strengthening the research on the environmental aspects of novel processes.

(4) Currently, carbon emission models are still at the theoretical stage and have not been integrated into intelligent green machining nor applied in actual factory processes. Therefore, their contribution to intelligent machining in factories is limited. Future research should focus on the practical application of carbon emission models in smart factories to provide guidance for intelligent and environmentally friendly production.

Nomenclature

Abbreviations

CAT	Cryogenic assisted turning
CBAM	Carbon border adjustment mechanism
CMQL	Cryogenic minimum quantity lubrication
CNC	Computer numerical control
CO_2	Carbon dioxide
CUAT	Cryogenic ultrasonic-assisted turning
EMQL	Electrostatic minimum quantity lubrication
Al-GnP	Alumina and graphene nanoplatelet
IPCC	Intergovernmental Panel on Climate Change
LCO_2	Liquid carbon dioxide
LN_2	Liquid nitrogen
MRR	Material removal rate
MQL	Minimum quantity lubrication
NMQL	Nanofluid minimum quantity lubrication
NSGA-II	Non-dominated sorting genetic algorithm II
RSM	Response surface methodology
SEC	Specific energy consumption

List of symbols

CE_c	Carbon emissions from cutting fluid consumption
CE_{elec}	Carbon emissions from electricity consumption
CE_f	Carbon emissions from chip recycling processing
CE_j	Carbon emissions from fixture wear
CE_k	Carbon emissions from tool wear
$CE_{material}$	Carbon emissions from material consumption
CE_{oil}	Carbon emissions from lubricating oil consumption
CE_{total}	Total carbon emissions from machining processes
CE_{waste}	Carbon emissions from waste disposal
E_a	Additional load power consumption
E_c	Cutting power consumption
E_{cl}	Power consumption of the cooling lubrication system
E_f	Feed power consumption
E_h	Power consumption of the hydraulic system

E_u	Idle power consumption
F_e	Carbon emission coefficient of electricity

Acknowledgements This research was financially supported by the following organizations: the National Natural Science Foundation of China (Grant Nos. 52475469, 52375447), the Shandong Provincial Natural Science Foundation, China (Grant Nos. ZR2024ME255 and ZR2024QE100), and the Special Fund of Taishan Scholars Project, China (Grant No. tsqn202211179).

Conflict of Interest Changhe LI is a member of the Editorial Board of *Frontiers of Mechanical Engineering*, who was excluded from the peer review and all editorial decisions related to the acceptance and publication of this article. Peer review was handled independently by the other editors to minimize bias.

References

1. Ge W W, Li H C, Cao H J, Li C C, Wen X H, Zhang C Y, Mativenga P. Welding parameters and sequences integrated decision-making considering carbon emission and processing time for multi-characteristic laser welding cell. Journal of Manufacturing Systems, 2023, 70: 1–17
2. Johnson J M F, Franzluebbers A J, Weyers S L, Reicosky D C. Agricultural opportunities to mitigate greenhouse gas emissions. Environmental Pollution, 2007, 150(1): 107–124
3. Hansen J, Sato M. Greenhouse gas growth rates. Proceedings of the National Academy of Sciences of the United States of America, 2004, 101(46): 16109–16114
4. Sabine C, Ciais P, Jones C, Canadell J G. Ask the experts: the IPCC fifth assessment report. Carbon Management, 2014, 5(1): 17–25
5. Carbon Monitor. Global Daily Carbon Dioxide Emissions Report 2023. Carbon Emission Accounts and Datasets. 2023
6. Yoon H S, Lee J Y, Kim H S, Kim M S, Kim E S, Shin Y J, Chu W S, Ahn S H. A comparison of energy consumption in bulk forming, subtractive, and additive processes: review and case study. International Journal of Precision Engineering and Manufacturing-Green Technology, 2014, 1(3): 261–279
7. Ge W W, Cao H J, Li H C, Zhang C Y, Li C C, Wen X H. Multi-feature driven carbon emission time series coupling model for laser welding system. Journal of Manufacturing Systems, 2022, 65: 767–784
8. Jin M Z, Tang R Z, Ji Y J, Liu F, Gao L, Huisingh D. Impact of advanced manufacturing on sustainability: An overview of the special volume on advanced manufacturing for sustainability and low fossil carbon emissions. Journal of Cleaner Production, 2017, 161: 69–74
9. Salahi N, Jafari M A. Energy-performance as a driver for optimal production planning. Applied Energy, 2016, 174: 88–100
10. Fang K, Uhan N, Zhao F, Sutherland J W. A new approach to scheduling in manufacturing for power consumption and carbon footprint reduction. Journal of Manufacturing Systems, 2011, 30(4): 234–240
11. He B, Yu Q Y. Product sustainable design for carbon footprint during product life cycle. Journal of Engineering Design, 2021, 32(9): 478–495
12. Du H B, Li B L, Brown M A, Mao G Z, Rameezdeen R, Chen H. Expanding and shifting trends in carbon market research: a quantitative bibliometric study. Journal of Cleaner Production, 2015, 103: 104–111
13. Haddad Y, De Bonneval E G, Afy-Shararah M, Carter J, Artingstall J, Salonitis K. Energy flexibility in aerospace manufacturing: The case of low carbon intensity production. Journal of Manufacturing Systems, 2024, 74: 812–825
14. Tu R H. Introduction to united nations framework convention on climate change and its Kyoto Protocol and their negotiation process. Environmental Protection, 2005, 36: 65–71 (in Chinese)
15. Kong L, Wang L M, Li F Y, Lv X T, Li J F, Ma Y, Chen B, Guo J. Multi-layer integration framework for low carbon design based on design features. Journal of Manufacturing Systems, 2021, 61: 223–238
16. Jeffry L, Ong M Y, Nomanbhay S, Mofijur M, Mubashir M, Show P L. Greenhouse gases utilization: A review. Fuel, 2021, 301: 121017
17. Cao H J, Li H C. Dynamic Modelling of Carbon Flows in Manufacturing Systems and Carbon Efficiency Assessment Methods. Beijing: China Machine Press, 2022, 54–77
18. Cai W, Li L, Jia S, Liu C H, Xie J, Hu L K. Task-oriented energy benchmark of machining systems for energy-efficient production. International Journal of Precision Engineering and Manufacturing-Green Technology, 2020, 7(1): 205–218
19. Ge W W, Cao H J, Li H C, Zhang Q Z, Wen X H, Zhang C Y, Mativenga P. Data-driven carbon emission accounting for manufacturing systems based on meta-carbon-emission block. Journal of Manufacturing Systems, 2024, 74: 141–156

20. Jia S, Cai W, Liu C H, Zhang Z W, Bai S W, Wang Q Y, Li S S, Hu L K. Energy modeling and visualization analysis method of drilling processes in the manufacturing industry. Energy, 2021, 228: 120567
21. Khan S A, AI Rashid A, Muhammad J, Ali F, Koç M. 3D printing technology for rapid response to climate change: challenges and emergency needs. Intelligent and Sustainable Manufacturing, 2024, 1(1): 10004
22. Bhushan R K. Optimization of cutting parameters for minimizing power consumption and maximizing tool life during machining of Al alloy SiC particle composites. Journal of Cleaner Production, 2013, 39: 242–254
23. Zhu S, Zhang H, Jiang Z G, Cao H J. Multi-granularity dynamic model establishment and simulation of carbon emissions for machining process based on DEVS. Journal of Mechanical Engineering, 2018, 54(19): 158–169 (in Chinese)
24. Ball P D, Evans S, Levers A, Ellison D. Zero carbon manufacturing facility—towards integrating material, energy, and waste process flows. Proceedings of the Institution of Mechanical Engineers, Part B: Journal of Engineering Manufacture, 2009, 223(9): 1085–1096
25. Cao H J, Li H C, Du Y B, Li X G. Curent situation and development trend of low-carbon manufacture. Aeronautical Manufacturing Technology, 2012, 9: 26–31 (in Chinese)
26. Li H C, Cao H J, Liu L W, Xing B, Pan X, Wen X H, Ge W W. Research status and technology path of low-carbon manufacturing under the background of emission peak and carbon neutrality. Journal of Mechanical Engineering, 2023, 59(7): 225–240 (in Chinese)
27. Tridech S, Cheng K. Low carbon manufacturing: characterization, theoretical models and implementation. International Journal of Manufacturing Research, 2011, 6(2): 110–121
28. Jiang Z P, Gao D, Lu Y, Kong L H, Shang Z D. Quantitative analysis of carbon emissions in precision turning processes and industrial case study. International Journal of Precision Engineering and Manufacturing-Green Technology, 2021, 8(1): 205–216
29. Ding H, Guo D Y, Cheng K, Cui Q. An investigation on quantitative analysis of energy consumption and carbon footprint in the grinding process. Proceedings of the Institution of Mechanical Engineers, Part B: Journal of Engineering Manufacture, 2014, 228(6): 950–956
30. Yin R X, Cao H J, Li H C, Du Y B. Carbon emission quantification method of sand casting process and its application. Computer Integrated Manufacturing Systems, 2012, 18(5): 1071–1076 (in Chinese)
31. Liu F, Xu Z J, Dan B. Machining System Energy Characteristics and Their Applications. Beijing: China Machine Press, 1995, 55–79
32. Li W, Kara S. An empirical model for predicting energy consumption of manufacturing processes: a case of turning process. Proceedings of the Institution of Mechanical Engineers, Part B: Journal of Engineering Manufacture, 2011, 225(9): 1636–1646
33. Hu S H, Liu F, He Y, Hu T. An on-line approach for energy efficiency monitoring of machine tools. Journal of Cleaner Production, 2012, 27: 133–140
34. Balogun V A, Mativenga P T. Modelling of direct energy requirements in mechanical machining processes. Journal of Cleaner Production, 2013, 41: 179–186
35. Huang Z, Cao H J, Zeng D, Ge W W, Duan C M. A carbon efficiency approach for laser welding environmental performance assessment and the process parameters decision-making. The International Journal of Advanced Manufacturing Technology, 2021, 114(7–8): 2433–2446
36. Lin W W, Yu D Y, Zhang C Y, Zhang S Q, Tian Y H, Liu S Q, Luo M. Multi-objective optimization of machining parameters in multi-pass turning operations for low-carbon manufacturing. Proceedings of the Institution of Mechanical Engineers, Part B: Journal of Engineering Manufacture, 2017, 231(13): 2372–2383
37. Jiang X Y, Liu A, Yang G Z, Liu W J, Bian H Y, Suo Y Q. Low-carbon modeling and process parameter optimization in laser additive manufacturing process. Journal of Mechanical Engineering, 2022, 58(5): 223–238 (in Chinese)
38. Zhang C X, Liu C H, Zhao X. Optimization control method for carbon footprint of machining process. The International Journal of Advanced Manufacturing Technology, 2017, 92(5–8): 1601–1607
39. Yin R X, Cao H J, Li H C, Sutherland J W. A process planning method for reduced carbon emissions. International Journal of Computer Integrated Manufacturing, 2014, 27(12): 1175–1186
40. Cao H J, Li H C, Cheng H Q, Luo Y, Yin R X, Chen Y P. A carbon efficiency approach for life-cycle carbon emission characteristics of machine tools. Journal of Cleaner Production, 2012, 37: 19–28
41. Sihag N, Sangwan K S. An improved micro analysis-based energy consumption and carbon emissions modeling approach for a milling center. The International Journal of Advanced Manufacturing Technology, 2019, 104(1–4): 705–721
42. Cao H J, Li H C. Simulation-based approach to modeling the carbon emissions dynamic characteristics of manufacturing system considering disturbances. Journal of Cleaner Production, 2014, 64: 572–580
43. Song S L, Cao H J, Li H C. Evaluation method and application for carbon emissions of machine tools based on LCA. In: Proceedings of International Conference on Advanced Technology of Design and Manufacture (ATDM). Beijing: Institution of Engineering and Technology, 2010, 74–78
44. Li T, Kong L L, Zhang H C, Iqbal A. Recent research

and development of typical cutting machine tool's energy consumption model. Journal of Mechanical Engineering, 2014, 50(7): 102–111 (in Chinese)
45. Zhou G H, Zhang C, Lu F Y, Zhang J J. Integrated optimization of cutting parameters and tool path for cavity milling considering carbon emissions. Journal of Cleaner Production, 2020, 250: 119454
46. Wang Q L, Liu F. Mathematical model of multi-source energy flows for CNC machine tools. Journal of Mechanical Engineering, 2013, 49(7): 5–12 (in Chinese)
47. Mori M, Fujishima M, Inamasu Y, Oda Y. A study on energy efficiency improvement for machine tools. CIRP Annals, 2011, 60(1): 145–148
48. Dahmus J B, Gutowski T G. An environmental analysis of machining. In: Proceedings of the ASME 2004 International Mechanical Engineering Congress and Exposition. Manufacturing Engineering and Materials Handling Engineering. Anaheim: The American Society of Mechanical Engineers, 2004, 643–652
49. Khan A M, Jamil M, Mia M, He N, Zhao W, Gong L. Sustainability-based performance evaluation of hybrid nanofluid assisted machining. Journal of Cleaner Production, 2020, 257: 120541
50. Anderberg S E, Kara S, Beno T. Impact of energy efficiency on computer numerically controlled machining. Proceedings of the Institution of Mechanical Engineers, Part B: Journal of Engineering Manufacture, 2010, 224(4): 531–541
51. Khan A M, Gupta M K, Hegab H, Jamil M, Mia M, He N, Song Q H, Liu Z Q, Pruncu C I. Energy-based cost integrated modelling and sustainability assessment of Al-GnP hybrid nanofluid assisted turning of AISI52100 steel. Journal of Cleaner Production, 2020, 257: 120502
52. Hoghoughi M H, Farahnakian M, Elhami S. Environmental, economical, and machinability based sustainability assessment in hybrid machining process employing tool textures and solid lubricant. Sustainable Materials and Technologies, 2022, 34: e00511
53. Liu Z J, Sun D P, Lin C X, Zhao X Q, Yang Y. Multi-objective optimization of the operating conditions in a cutting process based on low carbon emission costs. Journal of Cleaner Production, 2016, 124: 266–275
54. Zhang H, Deng Z H, Fu Y H, Lv L S, Yan C. A process parameters optimization method of multi-pass dry milling for high efficiency, low energy and low carbon emissions. Journal of Cleaner Production, 2017, 148: 174–184
55. Deng Z H, Lv L S, Li S C, Wan L L, Liu W, Yan C, Zhang H. Study on the model of high efficiency and low carbon for grinding parameters optimization and its application. Journal of Cleaner Production, 2016, 137: 1672–1681
56. Wang Q, Zhang D H, Chen B, Zhang Y, Wu B H. Energy consumption model for drilling processes based on cutting force. Applied Sciences, 2019, 9(22): 4801
57. Li L, Yan J H, Xing Z W. Energy requirements evaluation of milling machines based on thermal equilibrium and empirical modelling. Journal of Cleaner Production, 2013, 52: 113–121
58. Madanchi N, Thiede S, Gutowski T, Herrmann C. Modeling the impact of cutting fluid strategies on environmentally conscious machining systems. Procedia CIRP, 2019, 80: 150–155
59. Li C B, Cui L G, Liu F, Li L. Multi-objective NC machining parameters optimization model for high efficiency and low carbon. Journal of Mechanical Engineering, 2013, 49(9): 87–96 (in Chinese)
60. Zhang Y B, Li L Y, Cui X, An Q L, Xu P M, Wang W, Jia D Z, Liu M Z, Dambatta Y S, Li C H. Lubricant activity enhanced technologies for sustainable machining: Mechanisms and processability. Chinese Journal of Aeronautics, 2025, 38(6): 103203
61. Guo D Y, Cheng K, Ding H, Yan J H, Ma Y H. An investigation on quantitative analysis of carbon footprint in centreless grinding process and its key factors. China Mechanical Engineering, 2014, 25(11): 1478–1485
62. Wang Y L, Zhang Y B, Cui X, Liang X L, Li R Z, Wang R X, Sharma S, Liu M Z, Gao T, Zhou Z M, Wang X M, Dambatta Y S, Li C H. High-speed grinding: from mechanism to machine tool. Advances in Manufacturing, 2025, 13(1): 105–154
63. Yi Q, Li C B, Tang Y, Chen X Z. Multi-objective parameter optimization of CNC machining for low carbon manufacturing. Journal of Cleaner Production, 2015, 95: 256–264
64. Cao W D, Ni J J, Jiang B Y, Ye C Q. A three-stage parameter prediction approach for low-carbon gear hobbing. Journal of Cleaner Production, 2021, 289: 125777
65. Zheng C W, Yan C P, Cao W D. Gear hobbing process carbon emission quantitative calculation model and its optimization. Modern Manufacturing Engineering, 2018, 457(10): 23–30 (in Chinese)
66. Khanna N, Kshitij G, Solanki M, Bhatt T, Patel O, Uysal A, Sarıkaya M. In pursuit of sustainability in machining thin walled α-titanium tubes: an industry supported study. Sustainable Materials and Technologies, 2023, 36: e00647
67. Munoz A A, Sheng P. An analytical approach for determining the environmental impact of machining processes. Journal of Materials Processing Technology, 1995, 53(3–4): 736–758
68. Cui X, Li C H, Yang M, Liu M Z, Gao T, Wang X M, Said Z, Sharma S, Zhang Y B. Enhanced grindability and mechanism in the magnetic traction nanolubricant grinding of Ti-6Al-4V. Tribology International, 2023, 186: 108603
69. Zhu D H, Zhang X M, Ding H. Tool wear

characteristics in machining of nickel-based superalloys. International Journal of Machine Tools and Manufacture, 2013, 64: 60–77
70. Chen M K, Zhang Y B, Liu B, Zhou Z M, Zhang N Q, Wang H H, Wang L Q. Design of intelligent and sustainable manufacturing production line for automobile wheel hub. Intelligent and Sustainable Manufacturing, 2024, 1(1): 10003
71. Jiang Z G, Zhou F, Zhang H, Wang Y, Sutherland J W. Optimization of machining parameters considering minimum cutting fluid consumption. Journal of Cleaner Production, 2015, 108: 183–191
72. Tian C L, Zhou G H, Zhang J J, Zhang C. Optimization of cutting parameters considering tool wear conditions in low-carbon manufacturing environment. Journal of Cleaner Production, 2019, 226: 706–719
73. Yin R X, Cao H J, Li H C. Carbon emission characteristics of mechanical manufacturing process based on functional description and its application. Computer Integrated Manufacturing Systems, 2014, 20(9): 2127–2133 (in Chinese)
74. Dang J Q, Wang H H, Wang C G, An Q L, Li Y G, Wang H W, Chen M. Microstructure evolution and surface strengthening behavior of 300M ultrahigh strength steel under engineered surface treatments. Materials Characterization, 2024, 215: 114127
75. Wei S S, Zhang J L, Zhang L, Zhang Y J, Song B, Wang X B, Fan J X, Liu Q, Shi Y S. Laser powder bed fusion additive manufacturing of NiTi shape memory alloys: a review. International Journal of Extreme Manufacturing, 2023, 5(3): 032001
76. Wu J Z, Sun J H, Zhang C Y, Cao H J, Ge W W. Carbon emission modeling and multi-response evaluation of fiber laser welding. Journal of Mechanical Engineering, 2023, 59(7): 186–199 (in Chinese)
77. Han W, Kong L B, Xu M. Advances in selective laser sintering of polymers. International Journal of Extreme Manufacturing, 2022, 4(4): 042002
78. Luo Y, Cao H J, Li H C, Cheng H Q. Carbon emission model and parameter optimization of CO_2 shielded welding based on GRNN. China Mechanical Engineering, 2013, 24(17): 2398–2403 (in Chinese)
79. Zheng J, Tang R Z. Carbon efficiency model and evaluation method for sand casting. Journal of Zhejiang University (Engineering Science), 2015, 49(1): 102–109
80. Yin R X. Carbon emission calculation of machining manufacturing process for normal machinery parts. Mechanical Engineer, 2018, 4: 8–11 (in Chinese)
81. Liu H L, Li B T, Tang W H. Manufacturing oriented topology optimization of 3D structures for carbon emission reduction in casting process. Journal of Cleaner Production, 2019, 225: 755–770
82. Peng T H, Cai X, Qu Z H, Tang A H, Shen R, Wang Q M, Yu W H. Research on calculation model of power supply carbon emission factor in regional power grid considering hierarchical and regional decoupling of large-scale power grid. Proceedings of the CSEE, 2024, 44(3): 894–905 (in Chinese)
83. Zhang Q Y, Qiao K, Hu C A, Su P, Cheng O Y, Yan N, Yan L H. Study on life-cycle carbon emission factors of electricity in China. International Journal of Low-Carbon Technologies, 2024, 19: 2287–2298
84. Jeswiet J, Kara S. Carbon emissions and CES™ in manufacturing. CIRP Annals, 2008, 57(1): 17–20
85. Yu L, Wang Y, Li D Z. Calculating and analyzing carbon emission factors of prefabricated components. Sustainability, 2023, 15(11): 8706
86. Panagiotopoulou V C, Stavropoulos P, Chryssolouris G. A critical review on the environmental impact of manufacturing: a holistic perspective. The International Journal of Advanced Manufacturing Technology, 2022, 118(1–2): 603–625
87. Hu X D, Zhang X M, Dong L, Li H J, He Z, Chen H H. Carbon emission factors identification and measurement model construction for railway construction projects. International Journal of Environmental Research and Public Health, 2022, 19(18): 11379
88. Mohebbi G, Bahadori-Jahromi A, Ferri M, Mylona A. The role of embodied carbon databases in the accuracy of life cycle assessment (LCA) calculations for the embodied carbon of buildings. Sustainability, 2021, 13(14): 7988
89. Dang J Q, Wang C G, Wang H H, An Q L, Wei J, Gao B, Liu Z M, Chen M. Deformation behavior and microstructure evolution of 300M ultrahigh strength steel subjected to high strain rate: an analytical approach. Journal of Materials Research and Technology, 2023, 25: 812–831
90. Zhang H P, Gao D. Analysis of influence factors of carbon dioxide emission during milling processes. Machine Building and Automation, 2013, 42(2): 29–31 (in Chinese)
91. Li C B, Tang Y, Cui L G, Li P Y. A quantitative approach to analyze carbon emissions of CNC-based machining systems. Journal of Intelligent Manufacturing, 2015, 26(5): 911–922
92. Zhang Y, Liu Q, Zhou Y D, Ying B S. Integrated optimization of cutting parameters and scheduling for reducing carbon emissions. Journal of Cleaner Production, 2017, 149: 886–895
93. Zhou G H, Zhou C, Lu Q, Tian C L, Xiao Z D. Feature-based carbon emission quantitation strategy for the part machining process. International Journal of Computer Integrated Manufacturing, 2018, 31(4–5): 406–425
94. Jiang Z P, Gao D, Lu Y, Liu X L. Optimization of cutting parameters for trade-off among carbon emissions, surface roughness, and processing time.

Chinese Journal of Mechanical Engineering, 2019, 32(1): 94
95. Cakir A K. A new approach to minimize carbon emission rate in turning processes. International Journal of Low Carbon Technologies, 2021, 16(4): 1444–1452
96. Günay M, Aslan E, Korkut İ, Şeker U. Investigation of the effect of rake angle on main cutting force. International Journal of Machine Tools and Manufacture, 2004, 44(9): 953–959
97. Tian C L, Zhou G H, Lu Q, Zhang J J, Xiao Z D, Wang R. An integrated decision-making approach on cutting tools and cutting parameters for machining features considering carbon emissions. International Journal of Computer Integrated Manufacturing, 2019, 32(7): 629–641
98. Hu L K, Tang R Z, He K Y, Jia S. Estimating machining-related energy consumption of parts at the design phase based on feature technology. International Journal of Production Research, 2015, 53(23): 7016–7033
99. Hu L K, Liu Y, Peng C, Tang W C J, Tang R Z, Tiwari A. Minimising the energy consumption of tool change and tool path of machining by sequencing the features. Energy, 2018, 147: 390–402
100. Feng C H, Chen X, Zhang J Y, Huang Y G, Qu Z B. Minimizing the energy consumption of hole machining integrating the optimization of tool path and cutting parameters on CNC machines. The International Journal of Advanced Manufacturing Technology, 2022, 121(1–2): 215–228
101. Li L, Deng X G, Zhao J H, Zhao F, Sutherland J W. Multi-objective optimization of tool path considering efficiency, energy-saving and carbon-emission for free-form surface milling. Journal of Cleaner Production, 2018, 172: 3311–3322
102. Wang J S, Duan G H, Li F Y, Yang X D, Zhang H C. Current situation and future developing trends of green manufacturing technology based on products' life cycle. Computer Integrated Manufacturing Systems, 1999, 5(4): 2–9 (in Chinese)
103. Zhou G H, Lu Q, Xiao Z D, Zhou C, Tian C L. Cutting parameter optimization for machining operations considering carbon emissions. Journal of Cleaner Production, 2019, 208: 937–950
104. He B, Hua Y C. Feature-based integrated product model for low-carbon conceptual design. Journal of Engineering Design, 2017, 28(6): 408–432
105. Tian Y Q, Yin R X. The grinding parameter optimization under the carbon benefit objective. Journal of Physics: Conference Series, 2023, 2561(1): 012016
106. Ic Y T, Saraloğlu Güler E, Cabbaroğlu C, Dilan Yüksel E, Maide Sağlam H. Optimisation of cutting parameters for minimizing carbon emission and maximising cutting quality in turning process. International Journal of Production Research, 2018, 56(11): 4035–4055
107. Li Y, Liu Q. Service-oriented research on multi-pass milling parameters optimization for green and high efficiency. Journal of Mechanical Engineering, 2015, 51(11): 89–98 (in Chinese)
108. Jiang Z P, Gao D, Lu Y, Shang Z D, Kong L H. Optimisation of cutting parameters for minimising carbon emissions and cost in the turning process. Proceedings of the Institution of Mechanical Engineers, Part C: Journal of Mechanical Engineering Science, 2022, 236(4): 1973–1985
109. Nguyen T T, Duong Q D, Mia M. Multi-response optimization of the actively driven rotary turning for energy efficiency, carbon emissions, and machining quality. Proceedings of the Institution of Mechanical Engineers, Part B: Journal of Engineering Manufacture, 2021, 235(13): 2155–2173
110. Zhang H P. Research on prediction techniques of carbon emission during NC milling processes. Thesis for the Master's Degree. Harbin: Harbin Institute of Technology, 2012, 23–56 (in Chinese)
111. Rajemi M F, Mativenga P T, Aramcharoen A. Sustainable machining: selection of optimum turning conditions based on minimum energy considerations. Journal of Cleaner Production, 2010, 18(10–11): 1059–1065
112. Zhong Q Q, Tang R Z, Peng T. Decision rules for energy consumption minimization during material removal process in turning. Journal of Cleaner Production, 2017, 140: 1819–1827
113. Huisingh D, Zhang Z H, Moore J C, Qiao Q, Li Q. Recent advances in carbon emissions reduction: policies, technologies, monitoring, assessment and modeling. Journal of Cleaner Production, 2015, 103: 1–12
114. Zhou L R, Li J F, Li F Y, Meng Q, Li J, Xu X S. Energy consumption model and energy efficiency of machine tools: a comprehensive literature review. Journal of Cleaner Production, 2016, 112: 3721–3734
115. Gutowski T, Murphy C, Allen D, Bauer D, Bras B, Piwonka T, Sheng P, Sutherland J, Thurston D, Wolff E. Environmentally benign manufacturing: observations from Japan, Europe and the United States. Journal of Cleaner Production, 2005, 13(1): 1–17
116. Shi J L, Liu F, Xu D J, Xie D. Power balance equation about the numerical control machine tool's main driver system driven by variable voltage variable frequency. Journal of Mechanical Engineering, 2010, 46(3): 118–124 (in Chinese)
117. Hu S H, Liu F, He Y, Hu T. No-load energy parameter characteristics of computerized numerical control machine tool main transmission system. Computer Integrated Manufacturing Systems, 2012, 18(2): 326–331 (in Chinese)

118. Weinert K, Inasaki I, Sutherland J W, Wakabayashi T. Dry machining and minimum quantity lubrication. CIRP Annals, 2004, 53(2): 511–537
119. Pusavec F, Krajnik P, Kopac J. Transitioning to sustainable production–Part I: application on machining technologies. Journal of Cleaner Production, 2010, 18(2): 174–184
120. Pimenov D Y, Mia M, Gupta M K, Machado A R, Tomaz Í V, Sarikaya M, Wojciechowski S, Mikolajczyk T, Kapłonek W. Improvement of machinability of Ti and its alloys using cooling-lubrication techniques: A review and future prospect. Journal of Materials Research and Technology, 2021, 11: 719–753
121. Dudzinski D, Devillez A, Moufki A, Larrouquère D, Zerrouki V, Vigneau J. A review of developments towards dry and high speed machining of Inconel 718 alloy. International Journal of Machine Tools and Manufacture, 2004, 44(4): 439–456
122. Diniz A E, de Oliveira A J. Optimizing the use of dry cutting in rough turning steel operations. International Journal of Machine Tools and Manufacture, 2004, 44(10): 1061–1067
123. Fratila D, Caizar C. Application of Taguchi method to selection of optimal lubrication and cutting conditions in face milling of AlMg3. Journal of Cleaner Production, 2011, 19(6–7): 640–645
124. Debnath S, Reddy M M, Pramanik A. Dry and near-dry machining techniques for green manufacturing. In: Gupta K (ed). Innovations in Manufacturing for Sustainability. Cham: Springer, 2019, 1–27
125. Davoodi B, Hosseini Tazehkandi A. Experimental investigation and optimization of cutting parameters in dry and wet machining of aluminum alloy 5083 in order to remove cutting fluid. Journal of Cleaner Production, 2014, 68: 234–242
126. Kara S, Li W. Unit process energy consumption models for material removal processes. CIRP Annals, 2011, 60(1): 37–40
127. Li X G, Yang Y, Li C B, Chen P, Cao H J. Analysis of carbon emission in gear dry machining process for green manufacturing. China Mechanical Engineering 2014, 25(16): 2184-2190 (in Chinese)
128. Shokrani A, Dhokia V, Muñoz-Escalona P, Newman S T. State-of-the-art cryogenic machining and processing. International Journal of Computer Integrated Manufacturing, 2013, 26(7): 616–648
129. Jouhara H, Chauhan A, Guichet V, Delpech B, Abdelkareem M A, Olabi A G, Trembley J. Low-temperature heat transfer mediums for cryogenic applications. Journal of the Taiwan Institute of Chemical Engineers, 2023, 148: 104709
130. Debnath S, Reddy M M, Yi Q S. Environmental friendly cutting fluids and cooling techniques in machining: a review. Journal of Cleaner Production, 2014, 83: 33–47
131. Wang D F, Dang J Q, Li Y G, Liu Z M, Wang H W, Chen M. Study on the surface integrity distribution of 300M ultrahigh strength steel subjected to different surface modification treatments. Surface and Coatings Technology, 2022, 451: 129033
132. Dubey V, Kumar Sharma A, Kumar Singh R. Study of various cooling methodology used in machining processes. Materials Today: Proceedings, 2020, 21: 1572–1576
133. Danish M, Ginta T L, Habib K, Carou D, Rani A M A, Saha B B. Thermal analysis during turning of AZ31 magnesium alloy under dry and cryogenic conditions. International Journal of Advanced Manufacturing Technology, 2017, 91(5–8): 2855–2868
134. da Silva F J, Franco S D, Machado Á R, Ezugwu E O, Souza A M. Performance of cryogenically treated HSS tools. Wear, 2006, 261(5–6): 674–685
135. Zhao X G, Hao X Q, Zhang Z H, An Q L, Sun H L, Li L, Chen M, He N. Low temperature CO_2 assisted PCD tool hard turning bearing ring device and experimental research. Surface Technology, 2023, 52(2): 307–316 (in Chinese)
136. Agrawal C, Wadhwa J, Pitroda A, Pruncu C I, Sarikaya M, Khanna N. Comprehensive analysis of tool wear, tool life, surface roughness, costing and carbon emissions in turning Ti–6Al–4V titanium alloy: Cryogenic versus wet machining. Tribology International, 2021, 153: 106597
137. Yildiz Y, Nalbant M. A review of cryogenic cooling in machining processes. International Journal of Machine Tools and Manufacture, 2008, 48(9): 947–964
138. Jamil M, Zhao W, He N, Gupta M K, Sarikaya M, Khan A M, R S M, Siengchin S, Pimenov D Y. R SM, Siengchin S, Pimenov DY. Sustainable milling of Ti–6Al–4V: A trade-off between energy efficiency, carbon emissions and machining characteristics under MQL and cryogenic environment. Journal of Cleaner Production, 2021, 281: 125374
139. Ross N S, Rai R, Ananth M B J, Srinivasan D, Ganesh M, Gupta M K, Korkmaz M E, Królczyk G M. Carbon emissions and overall sustainability assessment in eco-friendly machining of Monel-400 alloy. Sustainable Materials and Technologies, 2023, 37: e00675
140. Iqbal A, Suhaimi H, Zhao W, Jamil M, Nauman M M, He N, Zaini J. Sustainable milling of Ti-6Al-4V: Investigating the effects of milling orientation, cutter's helix angle, and type of cryogenic coolant. Metals, 2020, 10(2): 258
141. Zhang S, Li J F, Wang Y W. Tool life and cutting forces in end milling Inconel 718 under dry and minimum quantity cooling lubrication cutting conditions. Journal of Cleaner Production, 2012, 32: 81–87
142. Gu G Q, Wang D Z, Wu S J, Zhou S, Zhang B X. Research status and prospect of ultrasonic vibration and minimum quantity lubrication processing of nickel-

based alloys. Intelligent and Sustainable Manufacturing, 2024, 1(1): 10006
143. Cui X, Li C H, Ding W F, Chen Y, Mao C, Xu X F, Liu B, Wang D Z, Li H N, Zhang Y B, Said Z, Debnath S, Jamil M, Ali H M, Sharma S. Minimum quantity lubrication machining of aeronautical materials using carbon group nanolubricant: From mechanisms to application. Chinese Journal of Aeronautics, 2022, 35(11): 85–112
144. Kumar A, Sharma A K, Katiyar J K. State-of-the-art in sustainable machining of different materials using nano minimum quality lubrication (NMQL). Lubricants, 2023, 11(2): 64
145. Uysal A, Caudill J R, Schoop J, Jawahir I S. Minimising carbon emissions and machining costs with improved human health in sustainable machining of austenitic stainless steel through multi-objective optimisation. International Journal of Sustainable Manufacturing, 2020, 4(2–4): 281–299
146. Zhang F J, Li Z S, Cui W W. Development and application of OoW equipment for gear hobbing. Journal of Mechanical Transmission, 2023, 47(6): 139–147 (in Chinese)
147. Xu W H, Li C H, Cui X, Zhang Y B, Yang M, Gao T, Liu M Z, Wang X M, Zhou Z M, Sharma S, Dambatta Y S. Atomization mechanism and machinability evaluation with electrically charged nanolubricant grinding of GH4169. Journal of Manufacturing Processes, 2023, 106: 480–493
148. Shah P, Gadkari A, Sharma A, Shokrani A, Khanna N. Comparison of machining performance under MQL and ultra-high voltage EMQL conditions based on tribological properties. Tribology International, 2021, 153: 106595
149. Huang S Q, Lv T, Wang M H, Xu X F. Effects of machining and oil mist parameters on electrostatic minimum quantity lubrication–EMQL turning process. International Journal of Precision Engineering and Manufacturing-Green Technology, 2018, 5(2): 317–326
150. Huang S Q, Wang Z, Yao W Q, Xu X F. Tribological evaluation of contact-charged electrostatic spray lubrication as a new near-dry machining technique. Tribology International, 2015, 91: 74–84
151. Kashyap N, Rahman Rashid R A, Khanna N. Carbon emissions, techno-economic and machinability assessments to achieve sustainability in drilling Ti6Al4V ELI for medical industry applications. Sustainable Materials and Technologies, 2022, 33: e00458
152. Salvi H, Vesuwala H, Raval P, Badheka V, Khanna N. Sustainability analysis of additive + subtractive manufacturing processes for Inconel 625. Sustainable Materials and Technologies, 2023, 35: e00580
153. Khanna N, Shah P, Wadhwa J, Pitroda A, Schoop J, Pusavec F. Energy consumption and lifecycle assessment comparison of cutting fluids for drilling titanium alloy. Procedia CIRP, 2021, 98: 175–180
154. Liu G T, Li C H, Zhang Y B, Yang M, Jia D Z, Zhang X P, Guo S M, Li R Z, Zhai H. Process parameter optimization and experimental evaluation for nanofluid MQL in grinding Ti-6Al-4V based on grey relational analysis. Materials and Manufacturing Processes, 2018, 33(9): 950–963
155. Sun L Y, Zhang Y B, Cui X, An Q L, Chen Y, Jia D Z, Gong P, Liu M Z, Dambatta Y S, Li C H. Magnetic lubricants: preparation, physical mechanism, and application. Friction, 2025, early access, doi:10.26599/FRICT.2025.9441010
156. Song Y X, Li C H, Zhou Z M, Liu B, Sharma S, Dambatta Y S, Zhang Y B, Yang M, Gao T, Liu M Z, Cui X, Wang X M, Xu W H, Li R Z, Wang D Z. Nanobiolubricant grinding: a comprehensive review. Advances in Manufacturing, 2025, 13: 1–42
157. Song Y X, Xu Z L, Li C H, Zhou Z M, Liu B, Zhang Y B, Dambatta Y S, Wang D Z. Research progress on the grinding performance of nanobiolubricant minimum quantity lubrication. Surface Technology, 2023, 52(12): 1–19 (in Chinese)
158. Khan A M, Anwar S, Jamil M, Nasr M M, Gupta M K, Saleh M, Ahmad S, Mia M. Energy, environmental, economic, and technological analysis of Al-GnP nanofluid- and cryogenic LN_2-assisted sustainable machining of Ti-6Al-4V alloy. Metals, 2021, 11(1): 88
159. Gupta M K, Song Q H, Liu Z Q, Sarikaya M, Jamil M, Mia M, Singla A K, Khan A M, Khanna N, Pimenov D Y. Environment and economic burden of sustainable cooling/lubrication methods in machining of Inconel-800. Journal of Cleaner Production, 2021, 287: 125074
160. Cui X, Li C H, Zhang Y B, Said Z, Debnath S, Sharma S, Ali H M, Yang M, Gao T, Li R Z. Grindability of titanium alloy using cryogenic nanolubricant minimum quantity lubrication. Journal of Manufacturing Processes, 2022, 80: 273–286
161. Çetindağ H A, Çiçek A, Uçak N. The effects of CryoMQL conditions on tool wear and surface integrity in hard turning of AISI 52100 bearing steel. Journal of Manufacturing Processes, 2020, 56: 463–473
162. Yıldırım Ç V, Kıvak T, Sarıkaya M, Şirin Ş. Evaluation of tool wear, surface roughness/topography and chip morphology when machining of Ni-based alloy 625 under MQL, cryogenic cooling and CryoMQL. Journal of Materials Research and Technology, 2020, 9(2): 2079–2092
163. Dzido A, Krawczyk P, Badyda K, Chondrokostas P. Operational parameters impact on the performance of dry-ice blasting nozzle. Energy, 2021, 214: 118847
164. Jamil M, He N, Wei Z, Gupta M K, Khan A M. A novel quantifiable approach of estimating energy consumption, carbon emissions and cost factors in manufacturing of bearing steel based on triple bottom-line approach. Sustainable Materials and Technologies,

2023, 36: e00593

165. Khanna N, Agrawal C, Gupta M K, Song Q H, Singla A K. Sustainability and machinability improvement of Nimonic-90 using indigenously developed green hybrid machining technology. Journal of Cleaner Production, 2020, 263: 121402
166. Xu M R, Chen S, Kurniawan R, Li C P, Wei R, Teng H W, Kumaran T, Han P W, Ko T J. Machinability study of cryogenic-ultrasonic vibration-assisted milling Inconel 718 alloy. The International Journal of Advanced Manufacturing Technology, 2023, 127(9–10): 4887–4901
167. Dang J Q, An Q L, Lian G H, Zuo Z Y, Li Y G, Wang H W, Chen M. Surface modification and its effect on the tensile and fatigue properties of 300M steel subjected to ultrasonic surface rolling process. Surface and Coatings Technology, 2021, 422: 127566
168. Zhao B, You H X, Miao Q, Ding W F, Qian N, Xu J H. Surface integrity characterization of third-generation nickel-based single crystal blade tenons after ultrasonic vibration-assisted grinding. Chinese Journal of Aeronautics, 2025, 38(1): 103138
169. Cao Y, Ding W F, Zhao B, Wen X B, Li S P, Wang J Z. Effect of intermittent cutting behavior on the ultrasonic vibration-assisted grinding performance of Inconel718 nickel-based superalloy. Precision Engineering, 2022, 78: 248–260
170. Cao Y, Zhu Y J, Li H N, Wang C X, Su H H, Yin Z, Ding W F. Development and performance of a novel ultrasonic vibration plate sonotrode for grinding. Journal of Manufacturing Processes, 2020, 57: 174–186